THE JOURNAL OF PHYSICAL CHEMISTRY B

Feature Article

pubs.acs.org/JPCB

Hidden Scale Invariance in Condensed Matter

Jeppe C. Dyre*

DNRF Center "Glass and Time", IMFUFA, Department of Sciences, Roskilde University, P.O. Box 260, DK-4000 Roskilde, Denmark

ABSTRACT: Recent developments show that many liquids and solids have an approximate "hidden" scale invariance that implies the existence of lines in the thermodynamic phase diagram, so-called isomorphs, along which structure and dynamics in properly reduced units are invariant to a good approximation. This means that the phase diagram becomes effectively one-dimensional with regard to several physical properties. Liquids and solids with isomorphs include most or all van der Waals bonded systems and metals, as well as weakly ionic or dipolar systems. On the other hand, systems with directional bonding (hydrogen bonds or covalent bonds) or strong Coulomb forces generally do not exhibit hidden scale invariance. The article reviews the theory behind this picture of condensed matter and the evidence for it coming from computer simulations and experiments.

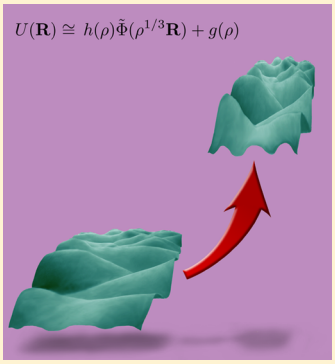

I. INTRODUCTION

The structure, dynamics, and thermodynamics of matter are generally well understood within a classical-mechanical framework, but at low temperatures quantum mechanics is of course required for a proper description. Although this subject by now is an established part of physical chemistry, there are intriguing hints of an underlying element of simplicity that is not yet fully understood. This section motivates the article by briefly reviewing the states of matter and listing some of the puzzles of contemporary condensed-matter physics and chemistry.

A. Three States of Matter. Matter comes in three states: gas, liquid, and solid.[1,2] The gas state is the simplest. Here its constituents move in straight lines most of the time, interrupted by violent collisions. This fact is responsible for a gas' structure, dynamics, and thermodynamics. If the gas consists of N atoms or molecules at temperature T, the ideal-gas relation between pressure p and volume V is $pV = Nk_BT$ in which $k_B = 1.38 \times 10^{-23}$ J/K is the Boltzmann constant. For all three states of matter, deviations from this equation are quantified by the so-called virial W giving the contribution to pressure from intermolecular interactions as follows

$$pV = Nk_BT + W \tag{1}$$

The virial is an extensive quantity of dimension energy.

The solid state is also fairly simple in regard to structure, dynamics, and thermodynamics. Thus, for most purposes a crystal is well represented as a regular lattice of atoms or molecules interacting via spring-like forces. Properties of equilibrium crystals traditionally in focus are lattice type and symmetry, phonon spectrum, elastic moduli, specific heat, etc. Equations of state of crystals are used mainly in connection with high-pressure studies. Here the noted Grüneisen equation of state expresses a linear relationship between pressure and energy E as follows (in which $\rho \equiv N/V$ is the atomic or molecular number density and the Grüneisen parameter γ_G only depends on the density)[3,4]

$$pV = \gamma_G(\rho)E + C(\rho) \tag{2}$$

$C(\rho)$ gives the energy-independent contribution to the pressure, which is responsible for a sizable fraction of the so-called cold pressure.[4]

The liquid state is complex. Like a solid, a liquid consists of strongly interacting atoms or molecules, but at the same time a liquid has the disorder and translational/rotational invariance of a gas. Early liquid-state research focused on properties like the viscosity and the equation of state.[5] In particular, via the Maxwell construction[6] the van der Waals equation of state gives rise to a simple theory of the liquid–gas transition. This equation also explains the existence of a critical point and the fact that liquid states can be continuously converted into gas states.[7]

The van der Waals equation emphasizes the liquid–gas resemblance. However, density and specific heat of liquids at ambient conditions are typically close to those of the corresponding crystal, not to their gas values. Back in the 1940s Frenkel wrote an entire book basically making the point that a liquid is more like a solid than like a gas.[8] Nowadays it is recognized that this is correct for the liquid phase not too far from the melting line, but not at high temperatures and fairly low pressures.[9] The focus below is on the former, "ordinary" liquid phase, which is quite different from the gas phase.[9,10] We refer to this and the crystalline/glass phases as condensed matter.[8,11]

B. Some Open Questions in the Physical Chemistry of Condensed Matter. A number of rules and correlations yet to be explained have been discovered in simulations and experiments on condensed matter. Intriguingly, these rules point to an element of simplicity, but likewise intriguingly they

Received: February 21, 2014
Revised: July 7, 2014
Published: July 11, 2014

   dx.doi.org/10.1021/jp501852b | J. Phys. Chem. B 2014, 118, 10007–10024

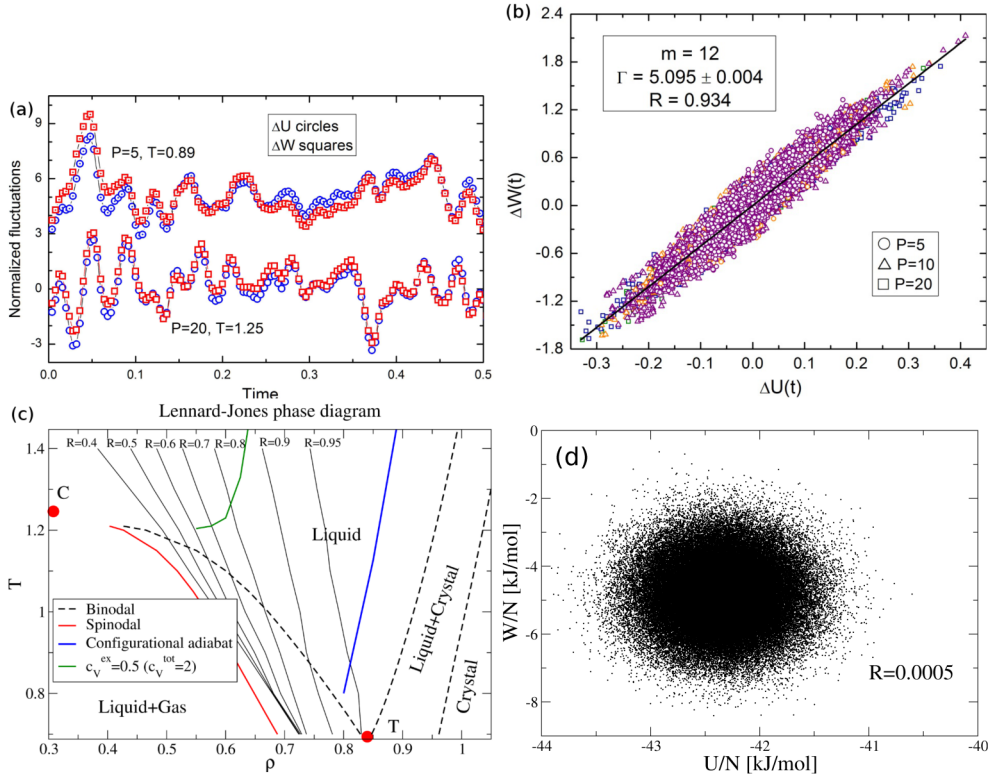

Figure 1. (a) Normalized thermal-equilibrium fluctuations of virial and potential energy as functions of time for two state points of a binary LJ-type system with an r^{-36} repulsive term. Reprinted with permission from D. Coslovich and C. M. Roland, *J. Chem. Phys.* **2009**, *130*, 014508. Copyright 2009, American Institute of Physics. (b) Scatter plots of virial and potential energies for the Kob–Andersen binary LJ system at three pressures; Γ is the slope of the best-fit line and *R* is given by eq 5. Reprinted with permission from D. Coslovich and C. M. Roland, *J. Chem. Phys.* **2009**, *130*, 014508. Copyright 2009, American Institute of Physics. (c) Contour plots of *R* in the density–temperature phase diagram for the single-component LJ system. T and C indicate the triple and critical points. The blue curve is a configurational adiabat (an isomorph). Reprinted with permission from N. P. Bailey et al., *J. Chem. Phys.* **2013**, *139*, 184506. Copyright 2013, American Institute of Physics. (d) Virial potential-energy scatter plot for the TIP5P water model at temperature 12.5 °C and density 1007.6 kg/m^3. Reprinted with permission from N. P. Bailey et al., *J. Chem. Phys.* **2008**, *129*, 184507. Copyright 2008, American Institute of Physics.

all have exceptions. Below some examples of the questions these rules give rise to are listed.

- What is the cause of the Lindemann melting criterion[12] according to which melting takes place when a crystal's vibrational mean-square displacement is a certain fraction of the nearest-neighbor distance? Why is this fraction pressure independent for a given substance? What explains the several other empirical melting and freezing rules,[12,13] and why are none of these universally valid? Do single-phase melting rules make sense at all, given that the melting point is determined by the equality of the liquid and solid free energies?
- Why do van der Waals bonded liquids and polymers obey power-law density scaling[14,15] according to which the average relaxation time is a function of ρ^γ/T with a system-specific exponent γ? Why do the same systems obey isochronal superposition,[16] the observation that the average relaxation time determines the entire relaxation time spectrum, and why do these findings not apply for hydrogen-bonded systems?
- What is the cause of the so-called excess-entropy scaling discovered by Rosenfeld in 1977,[17] according to which a liquid's relaxation time and diffusion constant in properly reduced units are functions of the excess entropy (the entropy minus that of an ideal gas at the same density and temperature)? What explains the exceptions to excess entropy scaling?
- Why are simple liquids' properties quasiuniversal? Why does quasiuniversality not apply to all monatomic systems of point-like particles interacting via radially symmetric, pairwise additive forces? Why do some such systems, in fact, exhibit quite complex behavior?
- We mention right away that none of these questions are fully answered in this paper. The picture argued below is that the above rules generally apply for systems with hidden scale invariance—and in many cases only for such systems.

II. VIRIAL POTENTIAL-ENERGY CORRELATIONS

Consider a system of N particles with coordinates $\mathbf{r}_1$, ..., $\mathbf{r}_N$. When rigid molecules are dealt with, $\mathbf{r}_i$ represents the center of mass as well as the orientation of molecule i. It is convenient to define the collective position vector by $\mathbf{R} \equiv (\mathbf{r}_1, ..., \mathbf{r}_N)$ in terms of which the potential energy is denoted by $U(\mathbf{R})$. The virial W of the general equation of state (eq 1) is the thermal average of the microscopic virial defined[18,19] by $W(\mathbf{R}) \equiv 1/3\sum_i \mathbf{r}_i \cdot \mathbf{F}_i$ where $\mathbf{F}_i$ is the force on the ith particle. Since $\mathbf{F}_i = -\nabla_i U$, the microscopic virial is given by

$$W(\mathbf{R}) = -\frac{1}{3}\mathbf{R}\cdot\nabla U(\mathbf{R}) \tag{3}$$

dx.doi.org/10.1021/jp501852b | J. Phys. Chem. B 2014, 118, 10007–10024

In the fall of 2006, Ulf Pedersen and co-workers of the *Glass and Time* group discovered that the equilibrium fluctuations of U and W correlate strongly for the Lennard-Jones (LJ) system at typical liquid state points.[20,21] Recall that the LJ pair potential $v(r)$ is defined[22] by

$$v(r) = 4\varepsilon\left[\left(\frac{r}{\sigma}\right)^{-12} - \left(\frac{r}{\sigma}\right)^{-6}\right] \tag{4}$$

This function has its minimum at $r = 2^{1/6}\sigma$ at which distance $v = -\varepsilon$. Figure 1 shows results from computer simulations of equilibrium virial potential-energy fluctuations at typical state points of various systems. Figure 1(a) follows these two quantities in normalized form as functions of time for a LJ-type system, (b) shows a *WU* scatter plot for the Kob–Andersen binary LJ liquid, (c) shows contours of constant correlation coefficient R (defined in eq 5 below) in the LJ phase diagram and, in particular, that the correlations are severely weakened as the critical point C is approached, and (d) shows results for a water model demonstrating very poor correlations. The simulations were all carried out at constant volume and temperature, in the so-called *NVT* ensemble.[19] In summary, strong *WU* correlations appear in many systems, but not universally.[23]

The correlation coefficient R is defined[23] by (where the sharp brackets denote *NVT* canonical averages and Δ the deviation from the average)

$$R \equiv \frac{\langle \Delta U \Delta W \rangle}{\sqrt{\langle (\Delta U)^2 \rangle \langle (\Delta W)^2 \rangle}} \tag{5}$$

As a consequence of Euler's theorem for homogeneous functions, perfect correlation ($R = 1$) is only possible for systems with a homogeneous potential-energy function,[24] i.e., one obeying $F(\lambda \mathbf{R}) = \lambda^{-n} F(\mathbf{R})$ for some exponent n. For the LJ liquid, typical values of R are 94–95%, whereas the crystalline face-centered cubic LJ crystal has $R > 99\%$.[25,26] The LJ correlation coefficient drops below 0.9 when negative-pressure states are approached, as well as when the critical point and gas states are approached[27] (compare Figure 1(c)).

An obvious idea for explaining the strong *WU* correlations of the LJ system is that these derive from the r^{-12} repulsive term of the pair potential. According to eq 3 that would lead to $\gamma = 12/3 = 4$ in the expression for the fluctuations

$$\Delta W \cong \gamma \Delta U \tag{6}$$

The observed γ values are, however, between 5.5 and 6 at typical moderate-pressure state points.[23,25] The solution to this puzzle is to note that the LJ pair potential is fitted well over the entire first coordination shell by the "extended IPL" (eIPL) function $a(r/\sigma)^{-n} + b + c(r/\sigma)$ with $n \cong 18$, not $n \cong 12$.[25] This reflects the fact that the attractive $(r/\sigma)^{-6}$ *term* of the LJ pair potential makes the repulsive *part* of the potential (below the minimum) much harsher than predicted from the $(r/\sigma)^{-12}$ term alone.[25,28−31] For constant-volume fluctuations the $c(r/\sigma)$ term contributes little to the W and U fluctuations because if a particle is moved, some of its nearest-neighbor distances decrease and some increase, with the result that their sum is almost unchanged.[25]

This explains the strong *WU* correlations for LJ-type systems but not why strong correlations are observed also in more complex systems like the Lewis–Wahnström *ortho*-terphenyl (OTP) model (three rigidly connected LJ spheres with a 75° bond angle[32,33]), the rigid-bond flexible LJ-chain model,[34] a seven-atom toluene model,[23] the slow degrees of freedom of an all-atom biomembrane model,[35,36] etc. This paper, however, focuses on the consequences of strong *WU* correlations, not their origin for which a general theory does not yet exist.

Simulations have shown that, as for water (Figure 1(d)), directional bonding destroys the *WU* correlations. Strong Coulomb interactions also weaken the correlations.[37,38] We originally used the term "strongly correlating system" when $R > 0.9$ is obeyed at the state point in question, but that name often gave rise to confusion with strongly correlated quantum systems. Alternatively, the term "Roskilde-simple system" or just "Roskilde (R) system" may be used,[27,39,40] reflecting the fact that, as shown below, these systems have a number of simple properties relating to their structure, dynamics, and thermodynamics (the term "simple liquid" traditionally means a pair-potential system[18,40]).

III. HIDDEN SCALE INVARIANCE

This section introduces the concept of hidden scale invariance, an approximate property that appears to apply for a sizable fraction of all condensed matter.

A. Excess Thermodynamic Quantities and Reduced Variables. Recall from statistical mechanics that the Helmholtz free energy is a sum of the ideal-gas term, $F_{id} = Nk_BT \ln(\rho\Lambda^3/e)$ in which $\Lambda \propto 1/\sqrt{T}$ is the thermal de Broglie wavelength, and the "excess" free energy term given by $\exp(-F_{ex}/k_BT) = \int \exp(-U(\mathbf{R})/k_BT)\mathrm{d}\mathbf{R}/V^N$.[18] Other thermodynamic quantities likewise separate into a sum of an ideal-gas and an excess term. For instance, there is an excess entropy $S_{ex} = -(\partial F_{ex}/\partial T)_V$ and an excess isochoric specific heat $C_{V,ex}$, and these two quantities are related by the usual relation $C_{V,ex} = (\partial S_{ex}/\partial \ln T)_V$. Note that $S_{ex} < 0$ because a liquid is always more ordered than an ideal gas at the same volume and temperature. According to eq 1 the excess pressure is W/V, which implies that $W/V = -(\partial F_{ex}/\partial V)_T$.

Hidden scale invariance and the isomorph theory refer to so-called reduced quantities, which are defined by reference to the following unit system. If m is the average particle mass, the length, energy, and time units, l_0, e_0, and t_0, are defined by

$$l_0 = \rho^{-1/3}$$
$$e_0 = k_BT$$
$$t_0 = \rho^{-1/3}\sqrt{m/k_BT} \tag{7}$$

In the present context l_0 and e_0 are more fundamental than the time unit t_0 because the latter changes if one switches to Brownian dynamics.[41]

We use a tilde to denote a reduced-unit quantity, i.e., one made dimensionless by dividing by the appropriate combination of the above units. For instance, the reduced collective position vector is given by

$$\tilde{\mathbf{R}} \equiv \rho^{1/3}\mathbf{R} \tag{8}$$

the reduced force on particle i by $\tilde{\mathbf{F}}_i \equiv \mathbf{F}_i/(e_0/l_0) = \rho^{-1/3}\mathbf{F}_i/k_BT$, the reduced shear viscosity by $\tilde{\eta} \equiv \eta/(\rho^{2/3}(mk_BT)^{1/2})$, the reduced instantaneous shear modulus by $\tilde{G}_\infty \equiv G_\infty/(\rho k_BT)$, the reduced free energy by $\tilde{F} \equiv F/k_BT$, etc. The reduced entropy and specific heats are obtained simply by dividing by k_B.

Consider the infinitesimal uniform expansion $\mathbf{R} \rightarrow (1 + d\lambda)\mathbf{R}$. The relative volume change is $dV/V = (1 + d\lambda)^3 - 1 = 3\,d\lambda$, implying that $d \ln \rho = d\rho/\rho = -dV/V = -3d\lambda$, i.e., $d\lambda = -(1/3)$

dx.doi.org/10.1021/jp501852b | J. Phys. Chem. B 2014, 118, 10007−10024

$d \ln \rho$. Since $d\mathbf{R} = d\lambda\mathbf{R}$, the change of the potential energy is given by $dU(\mathbf{R}) = d\lambda\mathbf{R}\cdot\nabla U(\mathbf{R}) = -(1/3)d \ln \rho\mathbf{R}\cdot\nabla U(\mathbf{R})$, thus by eq 3 $dU(\mathbf{R}) = d \ln \rho W(\mathbf{R})$. The reduced coordinate $\tilde{\mathbf{R}}$ does not change during a uniform expansion, so this implies that

$$W(\mathbf{R}) = \left(\frac{\partial U(\mathbf{R})}{\partial \ln \rho}\right)_{\tilde{\mathbf{R}}} \tag{9}$$

B. Mathematical Scale Invariance and the Approximate "Hidden" Scale Invariance. A mathematical function of one variable $\phi(x)$ is termed scale invariant if it is homogeneous, i.e., obeys $\phi(\lambda x) = \lambda^{-n}\phi(x)$ for some real number n. Putting $x = 1$ we get $\phi(\lambda) = \lambda^{-n}\phi(1)$, thus the power-law function $\phi(x) \propto x^{-n}$ is the only possibility. For functions of several variables homogeneity is defined from the analogous requirement $\phi(\lambda\mathbf{x}) = \lambda^{-n}\phi(\mathbf{x})$; in this case the class of homogeneous functions is much larger. Euler's theorem states that a function is homogeneous of degree $-n$ if and only if it obeys $\mathbf{x}\cdot\nabla\phi(\mathbf{x}) = -n\phi(\mathbf{x})$. Perfect *WU* correlation, i.e., $R = 1$ and equality in eq 6, thus implies that $U(\mathbf{R})$ is homogeneous with $n = 3\gamma$ (compare eq 3).

By definition[42] a statistical-mechanical system exhibits *hidden scale invariance* if it for certain functions of density $h(\rho)$ and $g(\rho)$ obeys

$$U(\mathbf{R}) \cong h(\rho)\tilde{\Phi}(\tilde{\mathbf{R}}) + g(\rho) \tag{10}$$

Here $\tilde{\Phi}$ is a dimensionless function of the dimensionless variable $\tilde{\mathbf{R}}$, i.e., a function that involves no lengths or energies. The approximate equality eq 10 defines when a system is a Roskilde (R) system at the state point in question. This is not required to apply for all (micro)configurations as long as it works for the *physically relevant* ones, i.e., those that are important for the structure and dynamics.

C. Consequences of Hidden Scale Invariance. The recently derived hidden-scale-invariance identity (eq 10) distills a number of previously identified properties of R systems into a single equation. This section shows that eq 10 implies (1) strong virial potential-energy correlations, (2) an expression for the "density-scaling exponent" γ of eq 6 in terms of $h(\rho)$, (3) the existence of isomorphs, (4) an equation for the isomorphic curves in the thermodynamic phase diagram, (5) a thermodynamic separation identity, and (6) a differential-geometric property.

Regarding the first two points, eqs 9 and 10 imply $W(\mathbf{R}) \cong (dh/d \ln \rho)\tilde{\Phi}(\tilde{\mathbf{R}}) + dg/d \ln \rho$. Eliminating $\tilde{\Phi}(\tilde{\mathbf{R}})$ in this expression leads to

$$W(\mathbf{R}) \cong \gamma(\rho)U(\mathbf{R}) + \phi(\rho) \tag{11}$$

in which

$$\gamma(\rho) = \frac{d \ln h}{d \ln \rho} \tag{12}$$

and $\phi(\rho) = -\gamma(\rho)g(\rho) + dg/d \ln \rho$. Note that eq 11 is the microscopic, configuration-space version of the Grüneisen equation of state (eq 2). Note also that eq 11 implies that a change of density results in the entire potential-energy surface simply undergoing a linear affine transformation (compare the figure in the abstract).

Averaging eq 11 at a given state point and subtracting this from eq 11 itself leads to $\Delta W(\mathbf{R}) \cong \gamma(\rho)\Delta U(\mathbf{R})$. Thus, hidden scale invariance implies strong correlations between the constant-volume equilibrium fluctuations of virial and potential energy (eq 6). Equation 11, however, also implies strong *WU* correlations for any nonequilibrium constant-volume situation.

Consider next two densities, ρ_1 and ρ_2, and two configurations at these densities, $\mathbf{R}_1$ and $\mathbf{R}_2$, with the same reduced coordinates, $\rho_1^{1/3}\mathbf{R}_1 = \rho_2^{1/3}\mathbf{R}_2 \equiv \tilde{\mathbf{R}}$. Then eq 10 implies $[U(\mathbf{R}_1) - g(\rho_1)]/h(\rho_1) \cong [U(\mathbf{R}_2) - g(\rho_2)]/h(\rho_2)$. If $K > 0$ and two temperatures are defined by $k_BT_1 \equiv h(\rho_1)/K$ and $k_BT_2 \equiv h(\rho_2)/K$, we get $U(\mathbf{R}_1)/k_BT_1 - Kg(\rho_1)/h(\rho_1) \cong U(\mathbf{R}_2)/k_BT_2 - Kg(\rho_2)/h(\rho_2)$. This means that for a number C_{12}, which depends on ρ_1 and ρ_2 but not on the configurations, one has

$$\exp\left(-\frac{U(\mathbf{R}_1)}{k_BT_1}\right) \cong C_{12}\exp\left(-\frac{U(\mathbf{R}_2)}{k_BT_2}\right) \tag{13}$$

Equation 13 implies identical canonical probabilities of configurations with the same reduced coordinates. By definition, two state points (ρ_1, T_1) and (ρ_2, T_2) are *isomorphic* whenever eq 13 applies for all their physically relevant configurations;[41] for molecular systems isomorphs are defined by scaling the centers of masses while keeping the molecules' sizes and orientations unchanged.[33] This defines a mathematical equivalence relation in the thermodynamic phase diagram, the equivalence classes of which are continuous curves termed "isomorphs".

The only systems that obey eq 13 with an equality sign for all configurations are those with a homogeneous potential-energy function, in which case $C_{12} = 1$. Realistic systems thus have only approximate isomorphs and $C_{12} \neq 1$. The latter fact is why $C(\rho)$ in eq 2 and $g(\rho)$ in eq 10 are never zero for realistic systems.

As a consequence of identical canonical probabilities, two isomorphic state points have the same excess entropy.[41] In other words, an isomorph is a configurational adiabat. Requiring identical canonical probabilities of pairs of scaled configurations is, however, much stronger than requiring identical excess entropy of two state points—all systems have configurational adiabats, but only some have isomorphs.

Since the constant K in the derivation of eq 13 determines the isomorph, the state points of an isomorph are given[43,44] by

$$\frac{h(\rho)}{k_BT} = K \tag{14}$$

Because K via the isomorph is a function of the excess entropy per particle, we can write $K = 1/f(s_{ex})$ and thus[43]

$$k_BT = f(s_{ex})h(\rho) \tag{15}$$

This thermodynamic separation identity is mathematically equivalent to the average of eq 11.[4,43]

The final characterization of R systems refers to their reduced-coordinate, constant-potential-energy hypersurfaces defined by $\tilde{\Omega} \equiv \{\tilde{\mathbf{R}} \mid U(\rho^{-1/3}\tilde{\mathbf{R}}) = \langle U\rangle\}$.[41,45] Generally, these high-dimensional compact Riemannian differentiable manifolds are parametrized by the two thermodynamic coordinates. For a system with hidden scale invariance, however, the $\tilde{\Omega}$-manifolds are characterized by just one parameter because eq 10 implies that

$$\tilde{\Omega} = \{\tilde{\mathbf{R}} \mid \tilde{\Phi}(\tilde{\mathbf{R}}) = \text{Const.}\} \tag{16}$$

D. Fundamental Isomorph Prediction: Invariance of Structure and Dynamics. If two state points (ρ_1, T_1) and (ρ_2, T_2) are isomorphic, they have the same structure and dynamics in reduced units (to a good approximation).[41] This result, which applies generally for both atomic and molecular systems,

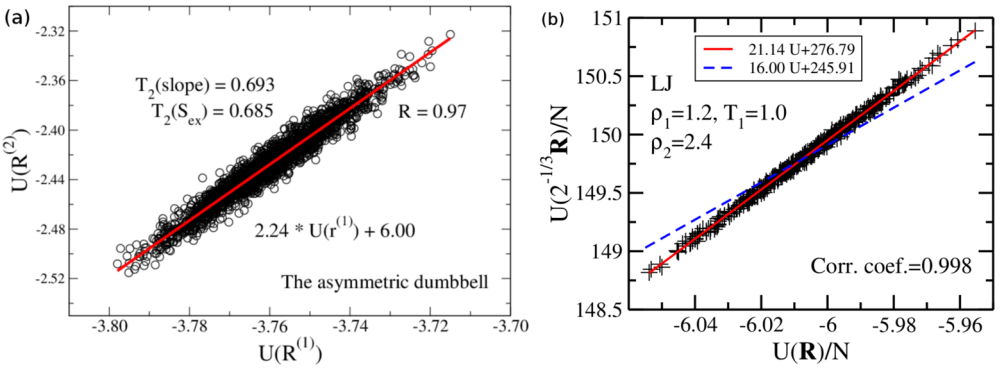

Figure 2. (a) Direct isomorph check method applied to the asymmetric dumbbell model (a large and a small LJ particle connected by a rigid bond). Simulations were carried out at $(\rho_1, T_1) = (0.868, 0.309)$ in LJ units from which all configurations were scaled to $\rho_2 = 0.999$. The isomorph temperature T_2 is calculated from the best-fit line slope as $T_2 = 2.24 * T_1 = 0.693$. Reprinted with permission from T. S. Ingebrigtsen et al., *J. Phys. Chem. B* **2012**, *116*, 1018. Copyright 2012. American Chemical Society. (b) The direct isomorph check applied to the LJ face-centered cubic crystal for a doubling of the density, starting at $\rho_1 = 1.2$ and $T_1 = 1$. In this case $T_2 = 21.14 * T_1 = 21.14$. The blue dashed line of slope 16 is the prediction of the repulsive r^{-12} term of the LJ potential. Reproduced from D. Albrechtsen et al., **2014**, arXiv:1406.1911. Published under CC license.

is for simplicity derived here only for an atomic system. First, we rewrite Newton's second law for the ith particle, $m_i\ddot{\mathbf{r}}_i = \mathbf{F}_i$, in terms of reduced coordinates. Defining by reference to eq 7 $\tilde{m}_i \equiv m_i/m$ where m is the average particle mass, $\tilde{\mathbf{r}}_i \equiv \mathbf{r}_i/l_0$, $\tilde{t} \equiv t/t_0$, and $\tilde{\mathbf{F}}_i \equiv \mathbf{F}_i/(e_0/l_0)$, Newton's law becomes $\tilde{m}_i\ddot{\tilde{\mathbf{r}}}_i = \tilde{\mathbf{F}}_i$ where the dots denote derivatives with respect to the reduced time. Likewise, in reduced coordinates the equipartition identity $m_i\langle\dot{\mathbf{r}}_i^2\rangle/2 = 3k_BT/2$ becomes $\tilde{m}_i\langle\tilde{\dot{\mathbf{r}}}_i^2\rangle/2 = 3/2$.

For all state points the equations of motion, as well as the average kinetic energy, thus have identical appearance when written in terms of reduced coordinates. This does not by necessity imply the same structure and dynamics, however, because at different state points the reduced force is generally *not* the same function of the reduced coordinates. However, for isomorphic state points this is the case: eq 13 implies $U(\mathbf{R}_1)/k_BT_1 = U(\mathbf{R}_2)/k_BT_2 + \text{Const.}$ for any two physically relevant configurations of the state points (ρ_1, T_1) and (ρ_2, T_2) with the same reduced coordinates. Since $\nabla_1 = (\rho_1/\rho_2)^{1/3}\nabla_2 = (l_0^{(2)}/l_0^{(1)})\nabla_2$, we find by application of $-\nabla_1$ to the above relation that $\mathbf{F}_1/e_0^{(1)} = (l_0^{(2)}/l_0^{(1)})\mathbf{F}_2/e_0^{(2)}$, i.e., $\tilde{\mathbf{F}}_1 = \tilde{\mathbf{F}}_2$. Thus, for isomorphic state points the reduced force is the same function of the reduced coordinates.

This finishes the proof that Newton's second law is isomorph invariant. It is straightforward to show that Brownian dynamics likewise is isomorph invariant.[41] The physics is that the atomic or molecular paths at isomorphic state points are (approximately) identical, except for uniform scalings of space and time. It follows that all measures of structure and dynamics in reduced units are isomorph invariant. This implies invariance of a number of quantities in reduced units, e.g., the excess entropy, the excess isochoric specific heat, the viscosity, the instantaneous shear modulus, normalized time-autocorrelation functions, etc. (for details, see ref 41). It is important to realize that not all reduced quantities are isomorph invariant; this follows from the fact that generally $g(\rho) \neq 0$ in eq 10. Examples of noninvariant quantities are the reduced free energy, pressure, and bulk modulus—in particular the reduced equation of state is not isomorph invariant.

E. Which Condensed-Matter Systems Exhibit Hidden Scale Invariance? Whether or not a system is a Roskilde system depends on the nature of the interactions involved.[46] On the basis of extensive computer simulations of various model systems we have suggested that most or all van der Waals bonded and metallic systems exhibit hidden scale invariance.[23,47] This is consistent with the generally recognized fact that systems dominated by van der Waals interactions or metallic systems are regular in their structure and dynamics and have few anomalies.[48] On the other hand, simulations reveal that hidden scale invariance is incompatible with directional interactions, so most or all hydrogen-bonded and covalently bonded systems are not expected to be Roskilde simple. The same applies for most or all strongly ionic or dipolar systems, whereas the isomorph theory does seem to work well for weakly ionic or dipolar systems.

How about polymeric systems and, more generally, systems with significant intramolecular degrees of freedom? Even such apparently complex systems may exhibit hidden scale invariance; in fact, for most polymers the fluctuations bear little signature of the chain-molecular structure. This indicates that van der Waals bonded polymers may generally exhibit hidden scale invariance; indeed recent simulations of the rigid-bond flexible LJ-chain model, a polymer toy model, show that it has nice isomorphs.[34]

The above wording was deliberately somewhat vague because more work is needed before a full overview is at hand. Part of this work is to identify the signatures of hidden scale invariance. This is the focus of the next section.

IV. EVIDENCE FOR HIDDEN SCALE INVARIANCE

This section presents direct and indirect evidence that a sizable fraction of condensed matter has the approximate symmetry we term hidden scale invariance. In simulations it is easy to check for this by calculating the virial potential-energy correlation coefficient R of eq 5 at the state points in question. This is not possible in experiments, where the evidence for hidden scale invariance is typically of an *a posteriori* nature.

First, we address the question how isomorphic state points are identified.

A. How to Identify Isomorphs? In simulations a safe, but somewhat tedious, method makes use of the fact that isomorphs are configurational adiabats; an example of an isomorph traced out in this way is the blue curve in Figure 1(c). In conjunction with the following identity for the γ of eqs 6 and 12[41]

dx.doi.org/10.1021/jp501852b | J. Phys. Chem. B 2014, 118, 10007−10024

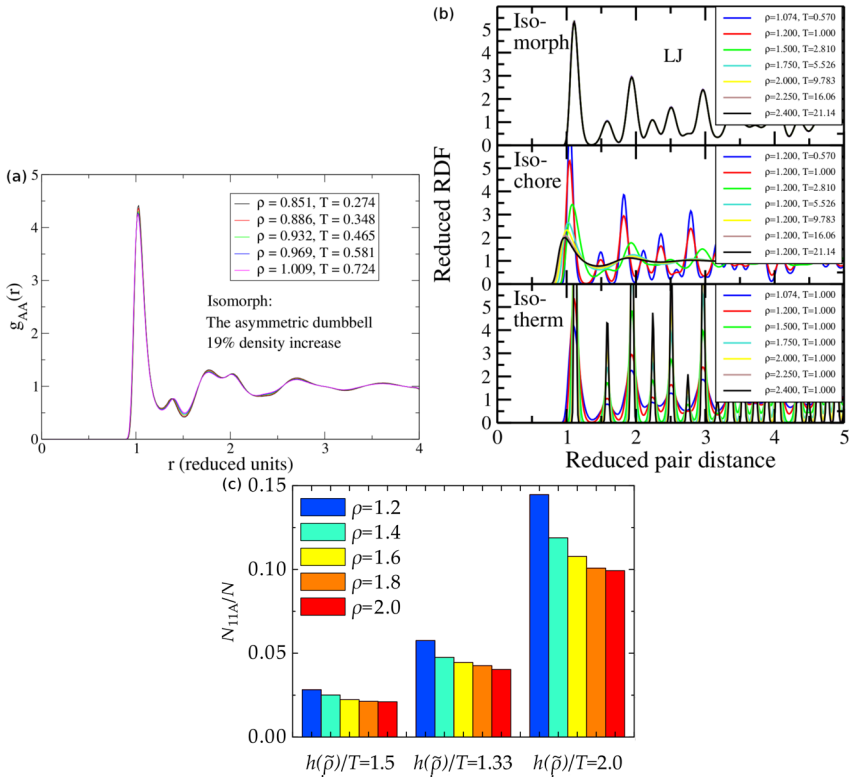

Figure 3. (a) Radial distribution function $g_{AA}(r)$ for the large (A) particles of the asymmetric dumbbell model along an isomorph. Reprinted with permission from T. S. Ingebrigtsen et al., *J. Phys. Chem. B* **2012**, *116*, 1018. Copyright 2012. American Chemical Society. (b) Radial distribution function for the face-centered cubic LJ crystal. The upper figure gives $g(r)$ for seven isomorphic state points with more than a factor of 2 density variation. The two lower figures show results for the corresponding isochores and isotherms. Reproduced from D. Albrechtsen et al., **2014**, arXiv:1406.1911. Published under CC license. (c) Occurrence of the so-called 11A bicapped square antiprism clusters, the prevalent structure in the KABLJ supercooled liquid, along three isomorphs. Reprinted with permission from A. Malins et al., *J. Chem. Phys.* **2013**, *139*, 234505. Copyright 2013, American Institute of Physics.

$$\gamma = \left(\frac{\partial \ln T}{\partial \ln \rho}\right)_{S_{ex}} = \frac{\langle \Delta W \Delta U \rangle}{\langle (\Delta U)^2 \rangle} \tag{17}$$

this is used as follows. At the initial state point the right-hand side is evaluated from an equilibrium *NVT* simulation. If density is increased, e.g., by 1%, the temperature increase required to arrive at the isomorphic state point is γ%. By iteration this may be continued indefinitely, but it is advisible to keep track of the correlation coefficient R in the process.

There are two "long-jump" methods allowing for larger density changes in simulations of systems with hidden scale invariance. One is the so-called direct isomorph check[41] that works as follows. Suppose the system is at the state point (ρ_1, T_1) and that one wishes to change density to ρ_2 isomorphically. For a simulation at (ρ_1, T_1) one plots $U[(\rho_1/\rho_2)^{1/3}\mathbf{R}_1]$ versus $U(\mathbf{R}_1)$ for several configurations. According to the logarithm of eq 13 the slope of the best fit line of the resulting scatter plot is T_2/T_1 (Figure 2). The direct isomorph check method is not fool proof, though. It runs into problems whenever $U(\mathbf{R}_1)$ and $U[(\rho_1/\rho_2)^{1/3}\mathbf{R}_1]$ are not highly correlated, which typically happens for large density changes. In that case consistency is not ensured, i.e., starting at (ρ_2, T_2) and making the reverse jump via the direct isomorph check, the temperature arrived at is not precisely T_1.

The second long-jump method is limited to atomic systems with pair potentials of the form $v(r) = \sum_n \varepsilon_n (r/\sigma)^{-n}$. For such systems the function $h(\rho)$ inherits the analytical structure of $v(r)$ in the sense that $h(\rho) = \sum_n \alpha_n \varepsilon_n (\rho\sigma^3)^{n/3}$.[43,44] For the LJ system, for instance, there are just two parameters in $h(\rho)$, α_6 and α_{12}. Since the overall normalization of $h(\rho)$ is arbitrary, only one of these needs to be determined, which is easily done from the fluctuations at a single state point by combining eqs 12 and 17.[43,44] Once $h(\rho)$ has been determined, the isomorphs are given by eq 14. This method generally works well,[43,44] but we have found that the highest accuracy is obtained when the function $h(\rho)$ is slightly modified from isomorph to isomorph.[49]

In experiments a configurational adiabat cannot be determined directly. For glass-forming liquids, which are highly viscous and have relaxation times that vary many orders of magnitude, isomorphs may be identified with the lines of constant relaxation time, the so-called isochrones. This is because the reduced relaxation time is an isomorph invariant, and the difference between reduced and real relaxation time is insignificant for such systems. In practice, viscous-liquid isochrones are often determined as the lines along which the dielectric loss-peak frequency is constant.[14−16,50] For less viscous liquids the viscosity is easier to measure. In this case isomorphs may be identified as curves of constant reduced viscosity; here the difference between real and reduced units cannot be ignored.[51−54]

B. Isomorph Invariance of Structure and Dynamics in Simulations. Figures 3 and 4 present simulation data showing that structure and dynamics to a good approximation are invariant along the isomorphs when given in reduced units. Figure 3(a) gives results for the reduced-unit radial distribution

dx.doi.org/10.1021/jp501852b | *J. Phys. Chem. B* 2014, 118, 10007−10024

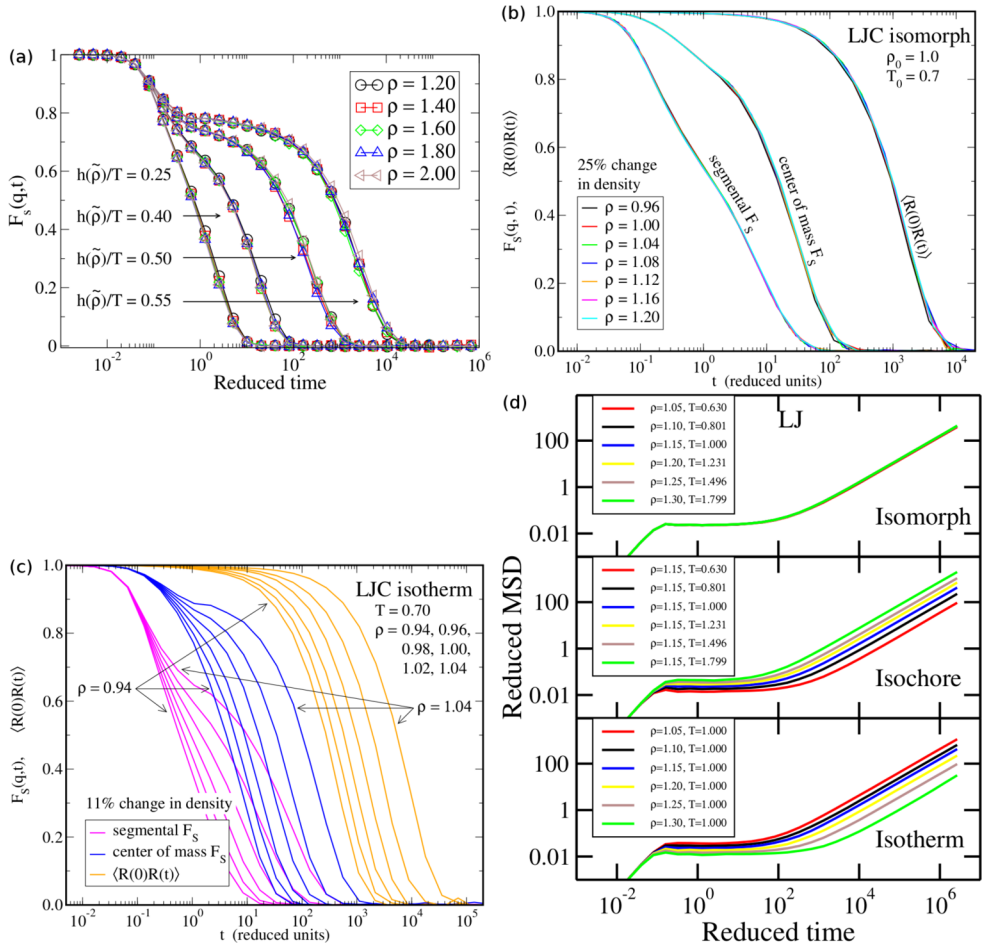

Figure 4. (a) Incoherent intermediate scattering function as a function of time for the large (A) particle of the KABLJ liquid along four isomorphs evaluated at the wavevector corresponding to the peak of $g(r)$. Reproduced from L. Bøhling et al., *New J. Phys.* **2012**, *14*, 113035. © 2012 IOP Publishing Ltd. and Deutsche Physikalische Gesellschaft. Published under a CC BY-NC-SA license. (b) and (c) The same quantity for the rigid-bond flexible LJ-chain (LJC) model with ten monomers, based on the segmental, center-of-mass, and end-to-end vectors, respectively. (b) Data along an isomorph and (c) data along an isotherm. Reproduced from A. A. Veldhorst et al., **2013**, arXiv:1307.5237. Published under CC license. (d) Atomic mean-square displacement as a function of time of a 1048 site face-centered cubic LJ crystal with eight atoms removed to allow for vacancy jump dynamics, along an isomorph, an isochore, and an isotherm. Reproduced from D. Albrechtsen et al., **2014**, arXiv:1406.1911. Published under CC license.

function of the large (A) particles of the asymmetric dumbbell model for five isomorphic state points. Clearly, the structure is invariant to a good approximation.

Approximate isomorph invariance has been demonstrated for the structure of many systems, including several LJ-type atomic liquids, the Buckingham-potential system, dumbbell systems, the Lewis–Wahnström OTP model, the rigid-bond flexible LJ chain model, etc.[20,23,33,34,38,55,105] Not surprisingly, the closer the correlation coefficient R is to unity, the better is the structure preserved along an isomorph. This is confirmed by Figure 3(b) showing data for the single-component face-centered cubic LJ crystal that generally has $R > 0.99$.[26]

How well isomorph invariance of the structure is obeyed depends on which structural characteristic is in focus. This is clear from Figure 3(c) that gives data for the occurrence of the prevalent local structure of the Kob–Andersen binary LJ (KABLJ) system.[56,57] Significant deviations from isomorph invariance are seen in particular at the lowest-pressure state point ($\rho = 1.2$).

Consider next the dynamics. Figure 4(a) shows simulation data for the incoherent intermediate scattering function as a function of time for the KABLJ system along four isomorphs. Figure 4(b) shows data for the rigid-bond flexible LJ-chain model's incoherent intermediate scattering functions of the segmental, center-of-mass, and end-to-end vectors, respectively, whereas Figure 4(c) shows analogous data along the isotherms. Finally, Figure 4(d) shows data for the dynamics of the LJ crystal with vacancy diffusion; isomorph invariance has also been demonstrated for the LJ crystal's phonon dynamics (data not shown).[26] Altogether, the dynamics is nicely isomorph invariant.

C. Density Scaling. Much of the experimental evidence for hidden scale invariance comes from studies of glass-forming liquids and polymers, which have extreme sensitivity of the dynamics to density and temperature. The evidence is based on the so-called power-law density-scaling relation,[14,15,58] which for a system with hidden scale invariance is justified as follows. Since density in most experiments varies by less than 10%, one can usually ignore the density dependence of γ. This amounts to making the approximation $h(\rho) \propto \rho^{\gamma}$ with a constant γ, which according to eq 14 implies that the isomorphs (isochrones) are given by $\rho^{\gamma}/T = \text{Const}$. This in turn implies that the (reduced) relaxation time is a function of ρ^{γ}/T. In analyzing experimental data, power-law density scaling is

dx.doi.org/10.1021/jp501852b | J. Phys. Chem. B 2014, 118, 10007–10024

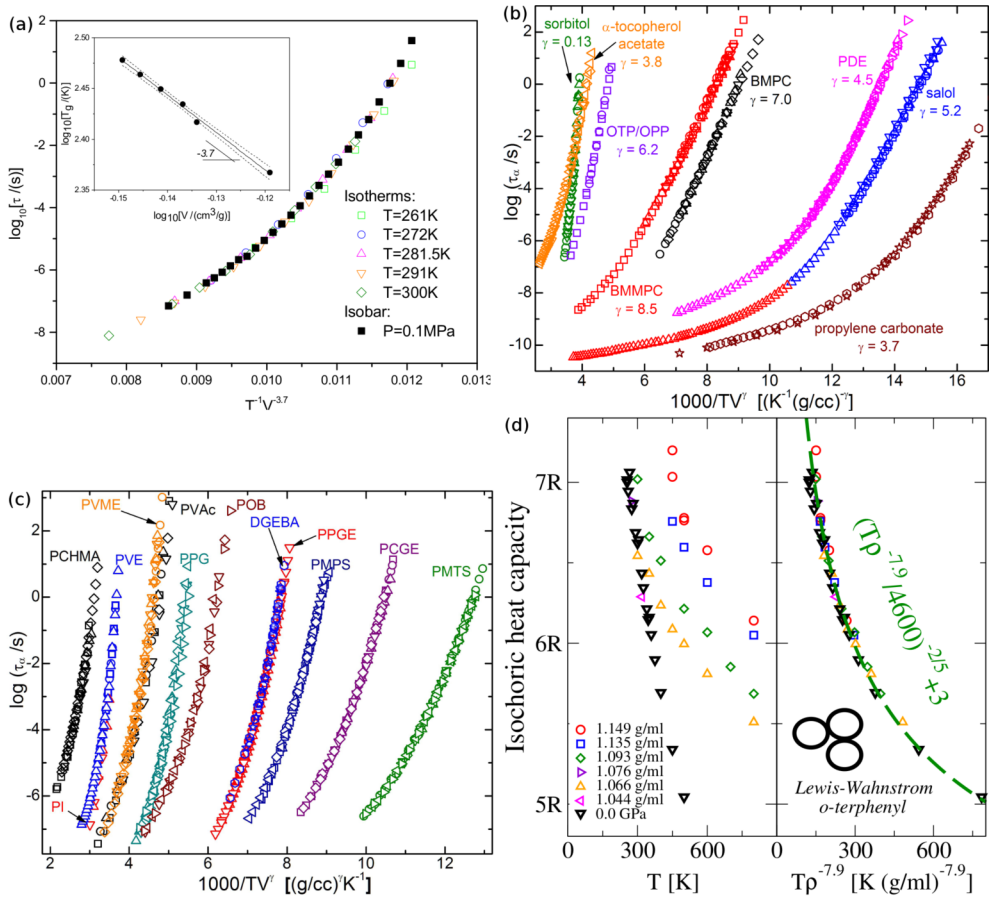

Figure 5. (a) Relaxation time data for the BMP-BB ionic liquid as a function of $1/(TV^{\gamma})$. Inset: The volume dependence of the glass-transition temperature used for determining γ (= 3.7). Reprinted with permission from M. Paluch et al., *J. Phys. Chem. Lett.* **2010**, *1*, 987. Copyright 2010. American Chemical Society. (b) and (c) Relaxation times for several small molecule and polymeric systems, respectively. For each system the density-scaling exponent γ was found by a best fit procedure; the data collapse shows that power-law density scaling applies. Reprinted with permission from C. M. Roland, *Macromolecules* **2010**, *43*, 7875. Copyright 2010. American Chemical Society. (d) Power-law density scaling of the heat capacity in simulations of Lewis–Wahnström OTP. Left: Raw data. Right: same data plotted as a function of T/ρ^{γ} in which γ = 7.9 was determined from the fluctuations at a single state point via eq 17. Reprinted from U. R. Pedersen et al., *J. Non-Cryst. Solids* **2011**, *357*, 320, Copyright 2011, with permission from Elsevier.

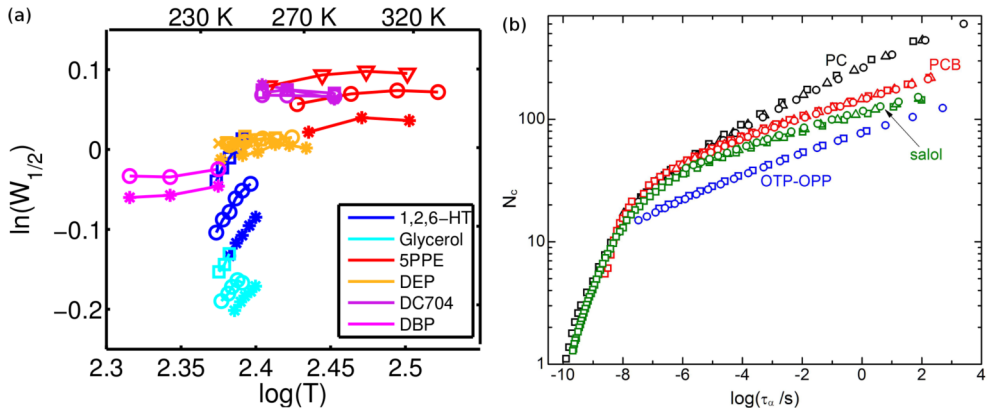

Figure 6. (a) Dielectric loss-peak half widths as functions of temperature along isochrones for six supercooled organic liquids. The blue symbols are hydrogen-bonding liquids, which are not expected to obey isochronal superposition according to which the half width is constant along an isochrone. The four other liquids are van der Waals bonded, expected to obey hidden scale invariance and thus isochronal superposition. Reprinted with permission from L. A. Roed et al., *J. Chem. Phys.* **2013**, *139*, 101101. Copyright 2013, American Institute of Physics. (b) Number of correlated molecules as a function of the relaxation time for four different systems at various temperatures and pressures ranging from ambient to 500 MPa. The observed collapse is predicted by the isomorph theory since both quantities are isomorph invariant. Reprinted with permission from D. Fragiadakis et al., *J. Phys. Chem. B* **2009**, *113*, 13134. Copyright 2009. American Chemical Society.

dx.doi.org/10.1021/jp501852b | *J. Phys. Chem. B* 2014, 118, 10007–10024

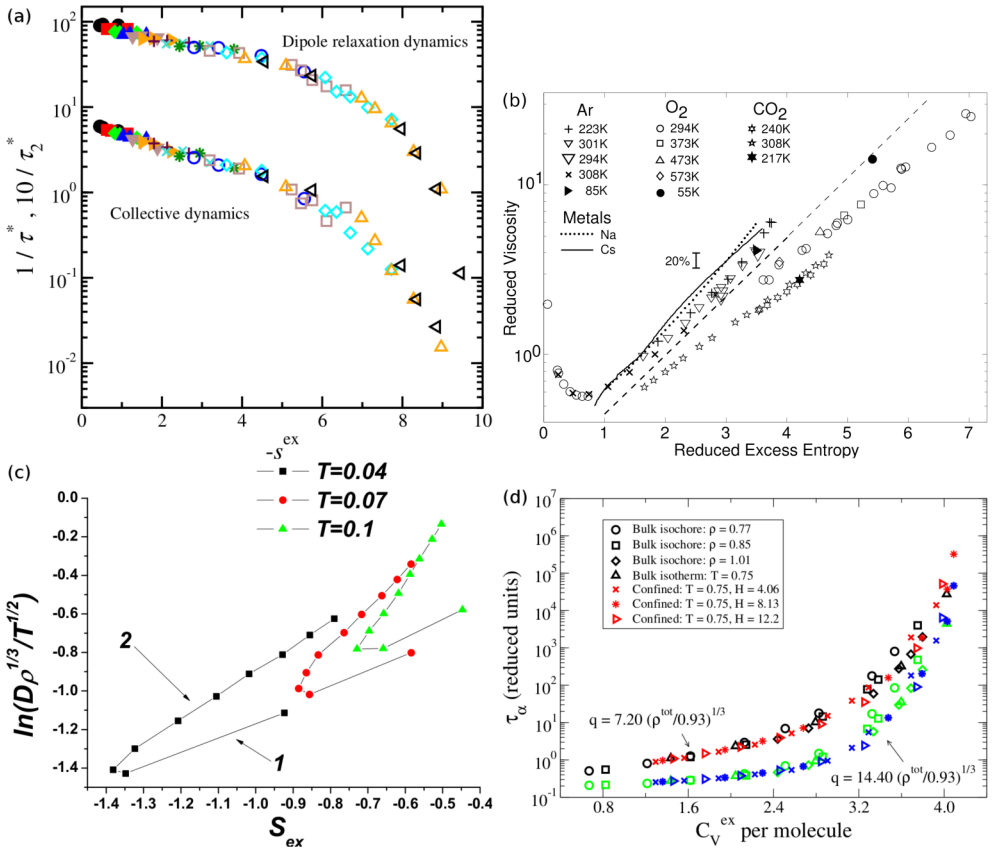

Figure 7. (a) Relaxation times derived from the orientational correlation function and the coherent intermediate scattering function of the symmetric dumbbell model as functions of the excess entropy. Reprinted with permission from R. Chopra et al., *J. Chem. Phys.* **2010**, *133*, 104506. Copyright 2010, American Institute of Physics. (b) Experimental data for the reduced viscosity at different temperatures and pressures plotted against excess entropy for five nonassociated systems. The metal data are taken along the liquid−vapor equilibrium line. The dashed line is the exponential entropy dependence Rosenfeld deduced from his 1977 computer simulations.[17] Reprinted with permission from E. H. Abramson and H. West-Foyle, *Phys. Rev. E* **2008**, *77*, 041202. Copyright 2008 by the American Physical Society. (c) Data for the reduced diffusion constant of the Gaussian-core model violating excess-entropy scaling. Reprinted with permission from Y. D. Fomin et al., *Phys. Rev. E* **2010**, *81*, 061201 (2010). Copyright 2010 by the American Physical Society. (d) Data for the relaxation time of the asymmetric dumbbell model, showing that the isochoric specific heat collapses data for different densities and temperatures (in confinement, as well as in the bulk). The two relaxation times plotted refer to different wavevectors of the incoherent intermediate scattering function. Reprinted with permission from T. S. Ingebrigtsen et al., *Phys. Rev. Lett.* **2013**, *111*, 235901. Copyright 2013 by the American Physical Society.

investigated by empirically determining whether or not an exponent γ exists that collapses data at different temperatures and pressures to be a function of the single variable ρ^γ/T.

Figure 5 shows experimental data validating power-law density scaling, where (a) shows data for a room-temperature ionic liquid, (b) for small-molecule liquids, and (c) for polymeric systems. That power-law density scaling also works in computer simulations is illustrated in Figure 5(d). In this case γ is not an empirical parameter but determined from eq 17 via a simulation at a single state point.

There are now experimental and simulation data demonstrating power-law density scaling for more than 100 different systems.[14,15] These include data for small-molecule systems, polymers, hydrocarbons,[51,59] liquid crystals,[60] etc. The general picture is that power-law density scaling works well for van der Waals bonded liquids and polymers but not for hydrogen-bonded systems.[14,15,58,61]

Interesting connections of density scaling to a system's elastic properties have been proposed,[62−65] but it should be mentioned that there are also theories connecting density scaling to excess-entropy scaling without invoking isomorphs.[66] Finally, we note that for large density changes, in experiments as well as in simulations, it is necessary to use the more general density-scaling relation eq 14.[44,61,67,68]

D. Isochronal Superposition. Isochronal superposition is the intriguing observation that when pressure and temperature are varied for many systems the average relaxation time determines the entire relaxation-time spectrum.[16,69,70] This is predicted by the isomorph theory because the invariance of dynamics implies that both the average (reduced) relaxation time and the relaxation-time spectrum are invariant along an isomorph; i.e., one determines the other. Computer simulation evidence for isochronal superposition is given in Figure 4, showing that the relaxation time spectrum is isomorph invariant, which implies in particular that the average relaxation time determines the spectrum. In experiments isochronal superposition has been found to apply for van der Waals bonded liquids and polymers, whereas hydrogen-bonded systems often disobey isochronal superposition[14,15,50] (Figure 6(a)). A related finding is that the number of correlated molecules in glass-forming van der Waals liquids (a quantity that is generally believed to increase upon cooling[71−74]) at different temperatures and pressures is a unique function of the

dx.doi.org/10.1021/jp501852b | J. Phys. Chem. B 2014, 118, 10007−10024

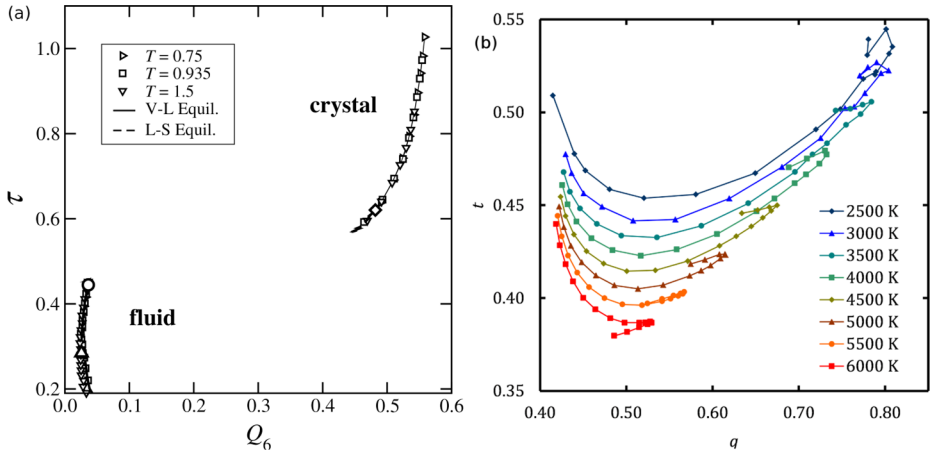

Figure 8. (a) Translational order parameter τ versus the orientational order parameter Q_6 for the LJ system. Both quantities are isomorph invariant, which explains the collapse. Reprinted with permission from J. R. Errington et al., *J. Chem. Phys.* **2003**, *118*, 2256. Copyright 2003, American Institute of Physics. (b) Translational order parameter t versus orientational order parameter q for a silica model in which case there is no collapse. Reprinted with permission from M. S. Shell et al., *Phys. Rev. E* **2002**, *66*, 011202. Copyright 2002 by the American Physical Society.

relaxation time.[58,75] Data confirming this are shown in Figure 6(b).

E. Excess Entropy Scalings. In 1977 Rosenfeld presented results from those times' fairly primitive computer simulations of a number of model liquids, showing that the reduced diffusion constant is a function of the excess entropy.[17] He justified what is now known as excess-entropy scaling by reference to the hard-sphere (HS) system: the fact that all reduced-unit properties of the HS system are uniquely determined by the packing fraction—a single number—implies excess-entropy scaling. For many years this intriguing discovery received limited attention, but in the past decade many more systems conforming to excess entropy scaling have been reported.[76−78] An example is given in Figure 7(a). Experimental data confirming excess-entropy scaling are given in Figure 7(b); there are similar data for nitrogen and methane.[79,80]

Not all systems conform to excess-entropy scaling. Exceptions are water models, the Gaussian core model (Figure 7(c)), the Hertzian model, the soft repulsive-shoulder-potential model, models with flexible molecules, etc.[40,81−87] Notably, these models all have poor virial potential-energy correlations. Indeed, for a Roskilde system, since both the excess entropy S_{ex} and the reduced diffusion constant $\tilde{D}$ are isomorph invariants, one *must* have $\tilde{D} = \tilde{D}(S_{ex})$. Thus, excess-entropy scaling is a consequence of hidden scale invariance. In this argument the excess entropy plays no special role, however, because any other isomorph-invariant quantity likewise predicts $\tilde{D}$ or the relaxation time. An example of this is provided in Figure 7(d), which shows that the specific heat C_V—another isomorph invariant[41]—"controls" the relaxation time of the asymmetric dumbbell system to a good approximation.

Interestingly, some systems without hidden scale invariance, e.g., Gaussian-core mixtures, the Widom−Rowlinson model, and hard-sphere mixtures, though violating classical Rosenfeld excess entropy scaling, conform to generalized excess-entropy scaling laws.[40,84,88,89] This shows that open questions remain in the rich area of exploring how excess entropy connects to the dynamics of complex fluids.

We finally note that Dzugutov in 1996 showed that the two-particle entropy S_2 predicts the dynamics of several model systems.[90] For R systems this follows from the fact that S_2 is an isomorph invariant.[41]

F. Order-Parameter Maps. Debenedetti and co-workers introduced a simple translational order parameter defined by $\int_0^{\tilde{r}_c} |g(\tilde{r}) - 1| d\tilde{r}$;[91,92] for orientational order different order parameters may be used. It turns out that for, e.g., the LJ system the translational order parameter uniquely determines the orientational order parameter (Figure 8(a)).[92] This is expected from the LJ system's hidden scale invariance because both order parameters are isomorph invariant. For water or silica models, on the other hand, there is no collapse (compare Figure 8(b)),[93−95] confirming that these are not R systems.

G. Thermoviscoelastic Response Functions and Unity Prigogine−Defay Ratio. Strong virial potential-energy correlations imply that the configurational parts of the pressure−pressure, pressure−energy, and energy−energy time correlation functions are (almost) proportional. Via the fluctuation−dissipation theorem this implies proportionality of the imaginary parts of different frequency-dependent thermoviscoelastic response functions[21,96] (compare the simulation data in Figure 9). From these imaginary parts it is possible to define a frequency-dependent Prigogine−Defay ratio, which is predicted to be close to unity for systems with hidden scale invariance.[21,96] In the classical theory of the glass transition, this corresponds to a so-called single-order-parameter description.[96−100]

Unfortunately, the relevant measurements are highly demanding.[101] A few data do exist, though, indicating that the dynamic Prigogine−Defay ratio is indeed closer to unity for van der Waals bonded liquids than for systems with hydrogen bonds or strong dipolar interactions.[102,103] Consistent with this it was shown by Casalini and Roland that power-law density scaling applies better the closer the standard "static" Prigogine−Defay ratio is to unity.[104]

H. Aging and Isomorph Jumps. The first papers on virial potential-energy correlations and isomorphs dealt with thermal-equilibrium states.[20,23,41] It turned out, however—as now predicted by eq 11—that strong *WU* correlations apply also for aging following a temperature jump or during crystallization (compare Figures 10(a) and (b)).

In a typical aging simulation one abruptly changes density and temperature to new values, after which the system gradually equilibrates. If such a jump takes place between two isomorphic

dx.doi.org/10.1021/jp501852b | J. Phys. Chem. B 2014, 118, 10007−10024

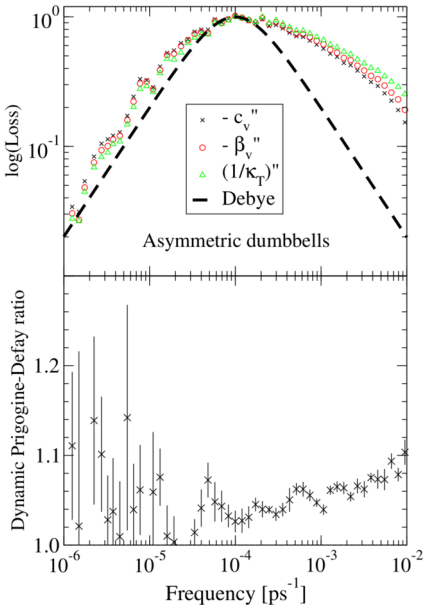

Figure 9. Upper figure: Imaginary parts of the frequency-dependent, negative isochoric specific heat, $-c_v''(\omega)$, negative pressure coefficient, $-\beta_v''(\omega)$, and inverse isothermal compressibility, $(1/\kappa_T)''(\omega)$, for the asymmetric dumbbell model. Lower figure: The corresponding dynamic Prigogine–Defay ratio defined by $\Lambda(\omega) \equiv -c_v''(\omega)\beta_v''(\omega)/[T\kappa_T''(\omega)(\beta_v''(\omega))^2]$ as a function of frequency, a quantity predicted to be unity at all frequencies for a perfect R system. Reprinted with permission from U. R. Pedersen et al., *Phys. Rev. E* **2008**, *77*, 011201. Copyright 2008 by the American Physical Society.

state points, it brings the system instantaneously to equilibrium because after the uniform scaling of all coordinates and adjustment of temperature, by eq 13 the states have the correct Boltzmann probabilities.[41] That this works in practice is illustrated for the rigid-bond flexible LJ-chain model in Figure 11(a). Such "isomorph jumps" have been performed in simulations of a number of atomic and molecular liquids and solids[26,33,41,105] but remain to be demonstrated in experiments.

For any system with hidden scale invariance a density–temperature jump can be thought of as a two-stage process. Immediately after the jump the structure is that of the new density's isomorphic temperature since the Boltzmann probabilities correspond to this temperature (eq 13). From here on, as illustrated in Figure 11(b), the system ages isochorically to the equilibrium state defined by the annealing temperature.

V. SOME FURTHER PROPERTIES OF SYSTEMS WITH HIDDEN SCALE INVARIANCE

The existence of isomorphs for Roskilde systems may be regarded as their "physical" characterization and the constant-potential-energy hypersurface characterization eq 16 as their "mathematical" characterization. There is also a third, "chemical" characterization: a system is an R system *if and only if* interactions beyond the first coordination shell (FCS) play little role for the system's structure and dynamics. This was the conclusion from the extensive numerical evidence presented in ref 47. We have no rigorous argument for this FCS characterization of R systems, although it has been shown to be consistent with the existence of isomorphs.[47] Interestingly, the roles of the second and further coordination shells have recently been discussed in relation to violations of excess entropy scaling.[106,107]

Some further implications of hidden scale invariance are

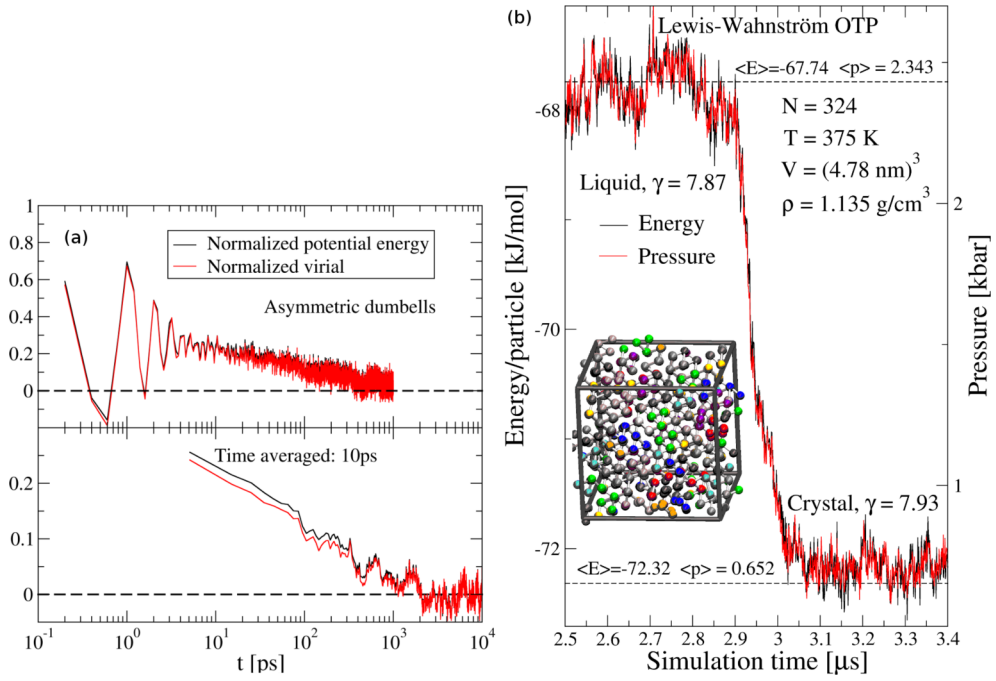

Figure 10. (a) Aging following a constant-density temperature down jump of the asymmetric dumbbell model, showing that virial potential-energy correlations are present also in out-of-equilibrium situations. Reprinted with permission from T. B. Schrøder et al., *J. Chem. Phys.* **2009**, *131*, 234503. Copyright 2009, American Institute of Physics. (b) Pressure and energy as functions of time during constant-volume crystallization of the Lewis–Wahnström OTP model. Reprinted with permission from T. B. Schrøder et al., *J. Chem. Phys.* **2009**, *131*, 234503. Copyright 2009, American Institute of Physics.

dx.doi.org/10.1021/jp501852b | *J. Phys. Chem. B* 2014, 118, 10007–10024

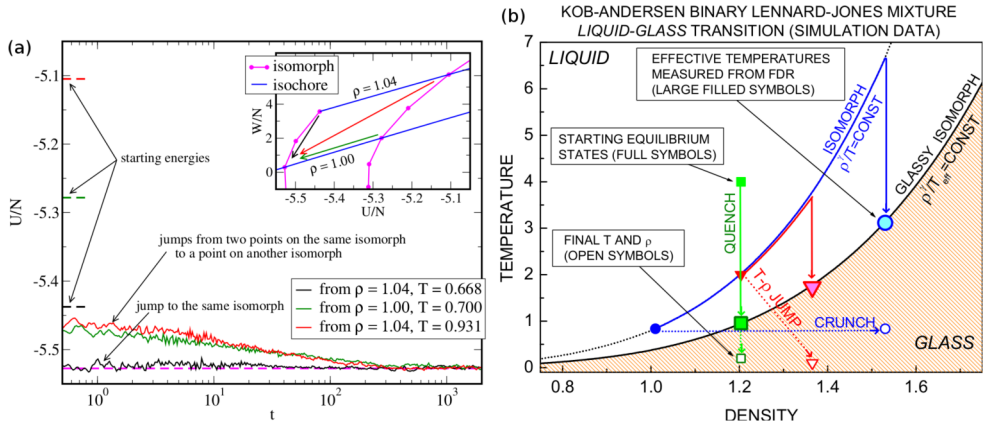

Figure 11. (a) Potential energy as a function of time following a jump in the phase diagram of the rigid-bond flexible LJ-chain model with ten monomers. After an isomorph jump the system is instantaneously in equilibrium (black curve), which is not the case for the two other jumps (red and green). Reproduced from A. A. Veldhorst et al., **2013**, arXiv:1307.5237. Published under CC license. (b) Aging scenarios for generic jumps. Following a change of density and temperature, the system initially has the structure corresponding to the new density and temperature isomorphic to the initial state point; subsequently the system ages isochorically (vertical arrows). Reprinted with permission from N. Gnan et al., *Phys. Rev. Lett.* **2010**, *104*, 125902. Copyright 2010 by the American Physical Society.

- Hidden scale invariance gives rise to an "isomorph filter" for general theories of viscous liquid dynamics, according to which the relaxation time must be controlled by an isomorph-invariant quantity.[41]
- The constant A of the Adam–Gibbs expression for the relaxation time of glass-forming liquids, $\tau \propto \exp(A/[TS_c(T)])$ in which S_c is the so-called configurational entropy,[108,109] was recently shown for the Kob–Andersen binary Lennard–Jones system to scale with density as required to make this expression isomorph invariant.[110]
- Roskilde systems obey the Rosenfeld–Tarazona expression for the excess isochoric heat capacity, $C_{V,ex} \propto T^{-2/5}$,[83,111] better than systems in general[112] (compare Figure 5(d)).
- The equation of state of experimental supercritical argon implies strong virial potential-energy correlations with correlation coefficient $R \cong 96\%$.[20,25]
- The concept of isomorphs may be extended to nanoconfined systems.[113]
- Isomorphs may be also defined for systems undergoing a steady-state, linear, or nonlinear shear flow.[114]
- The density dependence of the average stress of zero-temperature plastic flows follows the predictions of the power-law approximation to $h(\rho)$,[115−117] and recently the more general $h(\rho)$ scaling has been validated for the statistics of plastic flow events.[118]

An isomorph cannot cross the melting line because that would violate the condition of identical canonical probabilities of scaled configurations along the isomorph.[41] Thus, if the liquid and crystal phases both conform to hidden scale invariance, the system's isomorphs are parallel to the melting line on both sides of it, in the (p, T) as well as in the (ρ, T) phase diagrams—in the latter case there is an entire region of coexistence states, of course, the boundaries of which are both isomorphs.[41]

The fact that the freezing and melting lines in the (ρ, T) phase diagrams are isomorphs has a number of interesting consequences, for instance that the constant-volume melting entropy is pressure independent for a Roskilde system. Likewise, the reduced viscosity, the radial distribution function(s), etc., are invariant along the freezing line, and the Lindemann melting criterion is invariant along the melting line. Such regularities have been known for many years—in particular for metals and from simulations of various models—see, e.g., ref 13 and its references.

Single-phase melting or crystallization rules like the Lindemann criterion[12] are puzzling from a philosophical point of view because the melting curve is where the free energies of *two* phases are identical—how can one phase know about the free energy of the other? By referring to an isomorph invariant of a single phase, however, such criteria make good sense for R systems.

VI. OUTLOOK

A. Which Condensed-Matter Systems Are to Be Regarded As Simple? A liquid or solid system is traditionally defined as simple if it consists of point-like particles interacting via pairwise additive forces.[5,18,48,119−123] It has turned out from works of the last 10–20 years, however, that some such systems, e.g., the Gaussian core model and the Lennard–Jones Gaussian model,[124] have quite complex physics. These cases appear to always deal with systems of weak virial potential-energy correlations in the relevant part of the phase diagram,[13,42] whereas systems with hidden scale invariance to the best of the author's knowledge never have anomalies.

At the opposite extreme of the simplicity scale one finds water with its numerous anomalies[125] and $R \cong 0$ at typical state points.[20,23,24] The latter is a consequence of water's density maximum at which $(\partial p/\partial T)_V = 0$: if $(\partial W/\partial T)_V = 0$ then $R = 0$,[23] and since the main contribution to the thermal pressure coefficient is configurational,[25] water has $R \cong 0$ at ambient conditions. Thus, from the hidden-scale-invariance perspective, water's anomalous behavior is a consequence of its density maximum.

B. Roskilde-Simple Systems' Effectively One-Dimensional Thermodynamic Phase Diagram. The existence of isomorphs implies that the phase diagram is effectively one-dimensional with respect to all the isomorph invariant quantities. Since the thermodynamic phase diagram is two-dimensional, knowledge of a single isomorph invariant identifies the relevant isomorph, which implies knowledge of

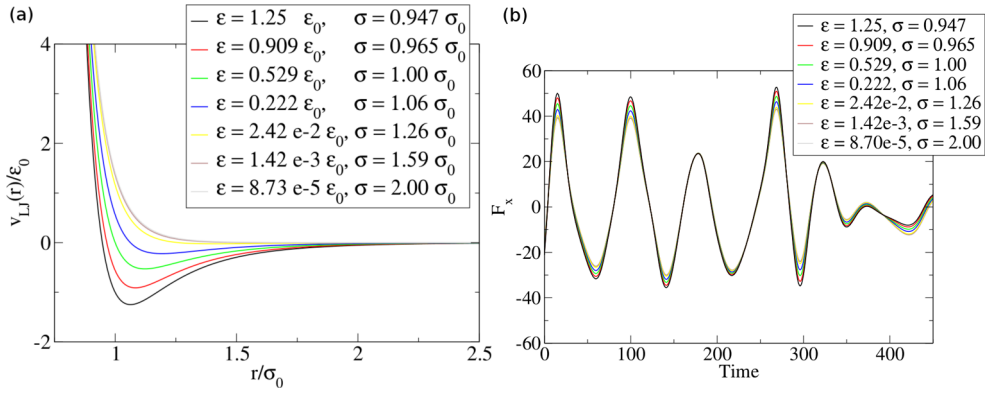

Figure 12. (a) Different LJ potentials predicted by the isomorph theory—and confirmed by simulations—to have the same physics to a good approximation. For some of these potentials the attractive forces are entirely insignificant. Reproduced by permission from L. Bøhling et al., *J. Phys.: Condens. Matter* **2013**, *25*, 032101. © 2013 IOP Publishing. All rights reserved. (b) The force on a particle as a function of time for the different LJ potentials evaluated along the same trajectory. Reproduced by permission from L. Bøhling et al., *J. Phys. Condens.: Matter* **2013**, *25*, 032101. © 2013 IOP Publishing. All rights reserved.

all other isomorph invariants. For instance, for systems with hidden scale invariance the excess entropy "controls" the dynamics no more than any other isomorph-invariant quantity, e.g., c_V (Figure 7(d)) or the reduced instantaneous shear modulus as in the shoving model.[126−128]

An effectively one-dimensional phase diagram is also a characteristic feature of the hard-sphere (HS) system which, because $U \equiv 0$, does not conform to hidden scale invariance in any reasonable sense of the term. The HS system is, however, a limit of such systems, namely the $n \rightarrow \infty$ limit of IPL systems. Combined with quasiuniversality[13] (section C below) the latter property explains why the excess entropy provides an accurate predictor of the HS system's dynamics and how it is affected by confinement.[129]

Berthier and Tarjus in 2009 opened an important discussion into the roles of the attractive and repulsive pair forces.[130,131] They did not dispute the conventional wisdom that the repulsive part of the pair potential controls the structure, but nevertheless demonstrated that ignoring the attractive pair forces gives a much too fast dynamics in the supercooled liquid state. In a continuation of this seminal work, however, the theory of hidden scale invariance leads one to question the standard paradigm of liquid-state theory according to which the attractive and repulsive forces play entirely different roles for the physics: Since the physics of any pair-potential system with $v(r) = \varepsilon\phi(r/\sigma)$ is a function of the two dimensionless variables $\rho\sigma^3$ and k_BT/ε, isomorph invariance may be reformulated to the statement that *different* pair potentials have the same physics at the *same* state point.[55] As an illustration, Figure 12(a) shows seven LJ potentials predicted to have the same structure and dynamics, a prediction that is validated by simulations.[55]

Why can quite different pair potentials define systems with almost identical structure and dynamics (although the pressure, of course, varies considerably)? The answer is that the potentials give rise to almost the same forces.[55] Thus, Figure 12(b) shows the x component of the force on one particle as a function of time for the different potentials, calculated along the same trajectory. The point is that it is the total force on a given particle that is relevant, not the individual pair forces—there is a lot of cancellation taking place when these are added vectorially.

C. Some Challenges and Open Problems. We finally discuss a few challenges and open problems, showing that more work is needed to get a full understanding of the causes and consequences of hidden scale invariance.

As regards challenges to the isomorph theory, in relation to power-law density scaling the theory predicts that the same exponent γ controls the relaxation time as the melting line. This was recently confirmed from experimental data for systems of rigid almost spherical molecules with no polar bonds but is not the case for some flexible and dipolar molecules, indicating that certain systems in the latter class do not conform to hidden scale invariance.[132]

Different density-scaling exponents have also been reported for the alpha relaxation time and for the Johari−Goldstein beta/excess wing relaxation times,[133,134] even for some van der Waals bonded liquids (other workers report identical exponents, though[135]). This contradicts the isomorph theory, meaning either that the systems in question are not Roskilde systems or that the secondary relaxation processes harbor the deviations from ideality known to exist whenever $R < 1$.

The most widely used measure of dynamic heterogeneity, $\chi_4(t)$ of the NpT ensemble, has been found not to be invariant along the isochrones for van der Waals systems,[136,137] apparently violating isomorph invariance of the dynamics. However, $\chi_4(t)$ is an ensemble-dependent quantity, and an isomorph invariant version of $\chi_4(t)$ exists that was recently found in experiment to be virtually constant along the isochrones.[138]

Open problems include the following:

- *Equations of state.* Isomorph invariants include reduced-unit temperature derivatives of the free energy but neither the free energy itself nor any of its volume derivatives. In particular, the reduced pressure is not an isomorph invariant. On the basis of this one does not expect the equation of state to reflect a given system's hidden scale invariance, but actually there are recent interesting suggestions to the contrary.[139−141] For LJ-type systems one can say a lot about the connection between W and U,[142] which results in an equation of state when combined with the Rosenfeld−Tarazona relation $C_{V,ex} \propto T^{-2/5}$.[112,142] A related unresolved issue is whether hidden scale invariance implies a principle of corresponding states.[5,18,143]
- *Excess-entropy scaling and generalizations.* Some systems obey generalized excess-entropy scaling laws without

dx.doi.org/10.1021/jp501852b | J. Phys. Chem. B 2014, 118, 10007−10024

exhibiting strong *WU* correlations and classical Rosenfeld excess-entropy scaling. Examples include polar liquids, chains of LJ particles connected by springs, Gaussian-core mixtures, the Widom−Rowlinson model, some tetrahedrally bonded systems, and hard-sphere mixtures.[78,81,84,88,89,144−146] Why is this? One possible explanation is that the hidden-scale-invariance identity eq 10 may be generalized by replacing the potential energy by a free-energy function defined by integrating out certain degrees of freedom, for instance harmonic springs that model the covalent bonds. If this free-energy function is denoted by $F(\mathbf{R}', \rho, T)$ in which $\mathbf{R}'$ is a coarse-grained configuration coordinate, the relevant generalization of eq 10 is $F(\mathbf{R}', \rho, T) \cong h(\rho, T)\tilde{\Phi}(\tilde{\mathbf{R}}') + g(\rho, T)$. Any systems for which this identity is obeyed will have "pseudoisomorphs" in its phase diagram of constant coarse-grained excess entropy given by $h(\rho, T)/T$ = Const. with many of the properties and invariants of genuine isomorphs; at the same time the system may have poor virial potential-energy correlations.

- *Quasiuniversality*. Quasiuniversality is the observation that the physics of many monatomic systems is roughly the same, an idea going back to Rosenfeld[17] that has recently been shown to apply also for stochastic dynamics.[147] In terms of hidden scale invariance, quasiuniversality is the statement that the function $\tilde{\Phi}$ of eq 10 is quasiuniversal: $\tilde{\Phi}(\tilde{\mathbf{R}}) \cong \tilde{\Phi}_0(\tilde{\mathbf{R}})$.[42] Recent works confirming quasiuniversality include studies of quasiuniversal melting criteria,[148] various LJ-type potentials,[149] plastic flow-event statistics,[118] and universally growing length scales upon supercooling.[39,150,151] The standard argument for quasiuniversality is based on representing the system in question by a HS reference system.[17,147,152−154] A recent alternative argument for quasiuniversality[13] refers to the so-called *NVU* dynamics, which is geodesic dynamics on the constant-potential-energy hypersurface.[45]
- *Which systems have hidden scale invariance?* Although it is straightforward in simulations to evaluate the *WU* correlation coefficient *R* at the state points in question, there is no theory for predicting *R*. And even when a Roskilde system has been identified, there is no general theory for calculating its scaling function $h(\rho)$. An exception to this is the case of monatomic pair-potential systems, for which it was recently shown that one has to a good approximation $h(\rho) \propto r_0^2 v''(r_0)$ evaluated at the most likely nearest-neighbor distance $r_0 \propto \rho^{-1/3}$.[49]
- *Do all systems become Roskilde simple at sufficiently high pressures?* On the basis of computer simulations we have conjectured that as $p \to \infty$ all systems eventually exhibit strong virial potential-energy correlations,[155] although simulations of a molten salt model appear to disprove the generality of this conjecture.[98] More work is needed to clarify the situation.

D. Concluding Remarks. The theory of hidden scale invariant systems does not fully answer any of the questions of section IB, but it throws new light on them. Thus, the rules involved in these questions appear to apply for all systems with hidden scale invariance. This indicates the potential significance of the class of Roskilde systems and the hidden-scale-invariance concept for getting a better understanding of the structure and dynamics of condensed matter.

AUTHOR INFORMATION

Corresponding Author

*E-mail: dyre@ruc.dk.

Notes

The author declares no competing financial interest.

Biography

Jeppe C. Dyre (b. 1956) is professor of physics at Roskilde University (Denmark). After studies of mathematics and physics at the University of Copenhagen, he has been with Roskilde University since 1984 from which he received his Ph.D. degree in theoretical physics. Originally interested in solid-state diffusion, ac electrical conduction in disordered solids, nonlinear response theory, and rheology, he has for many years worked on the physics of highly viscous liquids and the glass transition. Since 2005 he directs the theoretical and experimental DNRF center *Glass and Time*, the research of which has gradually expanded from focusing exclusively on glass-forming liquids to including the structure and dynamics of liquids and solids in general. Jeppe Dyre is a member of the Royal Danish Academy of Sciences and Letters.

ACKNOWLEDGMENTS

The author is indebted to his collaborators in theory development and simulations during the last several years, without whose enthusiastic work none of the developments summarized above would have taken place: Thomas Schrøder, Ulf Pedersen, Nick Bailey, Nicoletta Gnan, Søren Toxværd, Trond Ingebrigtsen, Lasse Bøhling, Jesper Schmidt Hansen, Arno Veldhorst, Lorenzo Costigliola, Andreas Olsen, Dan Albrechtsen, and Andreas Kvist Bacher. Jørgen Larsen and Heine Larsen are thanked for technical assistance in preparing this paper. The center for viscous liquid dynamics "Glass and Time" is sponsored by the Danish National Research Foundation's grant DNRF61.

REFERENCES

(1) Goodstein, D. L. *States of Matter*; Dover Publications: New York, 1985.

(2) Tabor, D. *Gases, Liquids and Solids: And other states of matter*, 3rd ed.; Cambridge University Press: United Kingdom, 1991.

(3) Born, M.; Huang, K. *Dynamical Theory of Crystal Lattices*; Oxford Univ. Press: United Kingdom, 1954.

(4) Nagayama, K. *Introduction to the Grüneisen Equation of State and Shock Thermodynamics*; Amazon Digital Services, Inc., 2011.

(5) Rowlinson, J. S.; Widom, B. *Molecular Theory of Capillarity*; Clarendon: Oxford, 1982.

(6) Atkins, P. W. *Physical Chemistry*, 4th ed.; Oxford Univ. Press: United Kingdom, 1990.

(7) Rowlinson, J. S. Legacy of van der Waals. *Nature* **1973**, *244*, 414−417.
(8) Frenkel, J. *Kinetic Theory of Liquids*; Clarendon: Oxford, 1946.
(9) Brazhkin, V. V.; Fomin, Y. D.; Lyapin, A. G.; Ryzhov, V. N.; Tsiok, E. N.; Trachenko, K. "Liquid-Gas" Transition in the Supercritical Region: Fundamental Changes in the Particle Dynamics. *Phys. Rev. Lett.* **2013**, *111*, 145901.
(10) Gorelli, F. A.; Bryk, T.; Krisch, M.; Ruocco, G.; Santoro, M.; Scopigno, T. Dynamics and Thermodynamics beyond the Critical Point. *Sci. Rep.* **2013**, *3*, 1203.
(11) Sidebottom, D. L. *Fundamentals of Condensed Matter and Crystalline Physics*; Cambridge University Press: United Kingdom, 2012.
(12) Ubbelohde, A. R. *Melting and Crystal Structure*; Clarendon: Oxford, 1965.
(13) Dyre, J. C. *NVU* Perspective on Simple Liquids' Quasiuniversality. *Phys. Rev. E* **2013**, *87*, 022106.
(14) Roland, C. M.; Hensel-Bielowka, S.; Paluch, M.; Casalini, R. Supercooled Dynamics of Glass-Forming Liquids and Polymers under Hydrostatic Pressure. *Rep. Prog. Phys.* **2005**, *68*, 1405−1478.
(15) Floudas, G.; Paluch, M.; Grzybowski, A.; Ngai, K. L. *Molecular Dynamics of Glass-Forming Systems: Effects of Pressure*; Springer: Berlin, 2011.
(16) Ngai, K. L.; Casalini, R.; Capaccioli, S.; Paluch, M.; Roland, C. M. Do Theories of the Glass Transition, in which the Structural Relaxation Time does not Define the Dispersion of the Structural Relaxation, Need Revision? *J. Phys. Chem. B* **2005**, *109*, 17356−17360.
(17) Rosenfeld, Y. Relation between the Transport Coefficients and the Internal Entropy of Simple Systems. *Phys. Rev. A* **1977**, *15*, 2545−2549.
(18) Hansen, J.-P.; McDonald, I. R. *Theory of Simple Liquids: With Applications to Soft Matter*, 4th ed.; Academic: New York, 2013.
(19) Allen, M. P.; Tildesley, D. J. *Computer Simulation of Liquids*; Oxford Science Publications: United Kingdom, 1987.
(20) Pedersen, U. R.; Bailey, N. P.; Schrøder, T. B.; Dyre, J. C. Strong Pressure-Energy Correlations in van der Waals Liquids. *Phys. Rev. Lett.* **2008**, *100*, 015701.
(21) Pedersen, U. R.; Christensen, T.; Schrøder, T. B.; Dyre, J. C. Feasibility of a Single-Parameter Description of Equilibrium Viscous Liquid Dynamics. *Phys. Rev. E* **2008**, *77*, 011201.
(22) Lennard-Jones, J. E. On the Determination of Molecular Fields. I. From the Variation of the Viscosity of a Gas with Temperature. *Proc. R. Soc. London A* **1924**, *106*, 441−462.
(23) Bailey, N. P.; Pedersen, U. R.; Gnan, N.; Schrøder, T. B.; Dyre, J. C. Pressure-Energy Correlations in Liquids. I. Results from Computer Simulations. *J. Chem. Phys.* **2008**, *129*, 184507.
(24) Schrøder, T. B.; Bailey, N. P.; Pedersen, U. R.; Gnan, N.; Dyre, J. C. Pressure-Energy Correlations in Liquids. III. Statistical Mechanics and Thermodynamics of Liquids with Hidden Scale Invariance. *J. Chem. Phys.* **2009**, *131*, 234503.
(25) Bailey, N. P.; Pedersen, U. R.; Gnan, N.; Schrøder, T. B.; Dyre, J. C. Pressure-Energy Correlations in Liquids. II. Analysis and Consequences. *J. Chem. Phys.* **2008**, *129*, 184508.
(26) Albrechtsen, D.; Olsen, A. E.; Pedersen, U. R.; Schrøder, T. B.; Dyre, J. C. Isomorph Invariance of Classical Crystals' Structure and Dynamics. 2014, arXiv:1406.1911.
(27) Bailey, N. P.; Bøhling, L.; Veldhorst, A. A.; Schrøder, T. B.; Dyre, J. C. Statistical Mechanics of Roskilde Liquids: Configurational Adiabats, Specific Heat Contours, and Density Dependence of the Scaling Exponent. *J. Chem. Phys.* **2013**, *139*, 184506.
(28) Stishov, S. M. The Thermodynamics of Melting of Simple Substances. *Sov. Phys. Usp.* **1975**, *17*, 625−643.
(29) Kang, H. S.; Lee, S. C.; Ree, T.; Ree, F. H. A Perturbation Theory of Classical Equilibrium Fluids. *J. Chem. Phys.* **1985**, *82*, 414−423.
(30) Ben-Amotz, D.; Stell, G. Analytical Implementation and Critical Tests of Fluid Thermodynamic Perturbation Theory. *J. Chem. Phys.* **2003**, *119*, 10777−10788.
(31) Coslovich, D.; Roland, C. M. Thermodynamic scaling of Diffusion in supercooled Lennard-Jones Liquids. *J. Phys. Chem. B* **2008**, *112*, 1329−1332.
(32) Lewis, L. J.; Wahnström, G. Molecular-Dynamics Study of Supercooled Ortho-Terphenyl. *Phys. Rev. E* **1994**, *50*, 3865−3877.
(33) Ingebrigtsen, T. S.; Schrøder, T. B.; Dyre, J. C. Isomorphs in Model Molecular Liquids. *J. Phys. Chem. B* **2012**, *116*, 1018−1034.
(34) Veldhorst, A. A.; Dyre, J. C.; Schrøder, T. B. Isomorph Scaling of Flexible Lennard-Jones Chains. 2013, arXiv:1307.5237.
(35) Pedersen, U. R.; Peters, G. H.; Schrøder, T. B.; Dyre, J. C. Volume-Energy Correlations in the Slow Degrees of Freedom of Computer-Simulated Phospholipid Membranes. *AIP Conf. Proc.* **2008**, *982*, 407−409.
(36) Pedersen, U. R.; Peters, G. H.; Dyre, J. C.; Schrøder, T. B. Correlated Volume-Energy Fluctuations of Phospholipid Membranes: A Simulation Study. *J. Phys. Chem. B* **2010**, *114*, 2124−2130.
(37) Ribeiro, M. C. C.; Scopigno, T.; Ruocco, G. Computer Simulation Study of Thermodynamic Scaling of Dynamics of $2Ca(NO_3)_2{\cdot}3KNO_3$. *J. Chem. Phys.* **2011**, *135*, 164510.
(38) Schrøder, T. B.; Pedersen, U. R.; Bailey, N. P.; Toxvaerd, S.; Dyre, J. C. Hidden Scale Invariance in Molecular van der Waals Liquids: A Simulation Study. *Phys. Rev. E* **2009**, *80*, 041502.
(39) Flenner, E.; Staley, H.; Szamel, G. Universal Features of Dynamic Heterogeneity in Supercooled Liquids. *Phys. Rev. Lett.* **2014**, *112*, 097801.
(40) Prasad, S.; Chakravarty, C. Onset of Simple Liquid Behaviour in Modified Water Models. *J. Chem. Phys.* **2014**, *140*, 164501.
(41) Gnan, N.; Schrøder, T. B.; Pedersen, U. R.; Bailey, N. P.; Dyre, J. C. Pressure-Energy Correlations in Liquids. IV. "Isomorphs" in Liquid Phase Diagrams. *J. Chem. Phys.* **2009**, *131*, 234504.
(42) Dyre, J. C. Isomorphs, Hidden Scale Invariance, and Quasiuniversality. *Phys. Rev. E* **2013**, *88*, 042139.
(43) Ingebrigtsen, T. S.; Bøhling, L.; Schrøder, T. B.; Dyre, J. C. Thermodynamics of Condensed Matter with Strong Pressure-Energy Correlations. *J. Chem. Phys.* **2012**, *136*, 061102.
(44) Bøhling, L.; Ingebrigtsen, T. S.; Grzybowski, A.; Paluch, M.; Dyre, J. C.; Schrøder, T. B. Scaling of Viscous Dynamics in Simple Liquids: Theory, Simulation and Experiment. *New J. Phys.* **2012**, *14*, 113035.
(45) Ingebrigtsen, T. S.; Toxvaerd, S.; Heilmann, O. J.; Schrøder, T. B.; Dyre, J. C. *NVU* dynamics. I. Geodesic Motion on the Constant-Potential-Energy Hypersurface. *J. Chem. Phys.* **2011**, *135*, 104101.
(46) Stone, A. *The Theory of Intermolecular Forces*, 2nd ed.; Oxford University Press: United Kingdom, 2013.
(47) Ingebrigtsen, T. S.; Schrøder, T. B.; Dyre, J. C. What Is a simple liquid? *Phys. Rev. X* **2012**, *2*, 011011.
(48) Chandler, D. *Introduction to Modern Statistical Mechanics*; Oxford University Press: United Kingdom, 1987.
(49) Bøhling, L.; Bailey, N. P.; Schrøder, T. B.; Dyre, J. C. Estimating the density-scaling exponent of a monatomic liquid from its pair potential. *J. Chem. Phys.* **2014**, *140*, 124510.
(50) Roed, L. A.; Gundermann, D.; Dyre, J. C.; Niss, K. Communication: Two Measures of Isochronal Superposition. *J. Chem. Phys.* **2013**, *139*, 101101.
(51) Galliero, G.; Boned, C.; Fernandez, J. Scaling of the Viscosity of the Lennard-Jones Chain Fluid Model, Argon, and some Normal Alkanes. *J. Chem. Phys.* **2011**, *134*, 064505.
(52) Fragiadakis, D.; Roland, C. M. On the Density Scaling of Liquid Dynamics. *J. Chem. Phys.* **2011**, *134*, 044504.
(53) Harris, K. R.; Kanakubo, M. High Pressure Studies of the Transport Properties of Ionic Liquids. *Faraday Discuss.* **2012**, *154*, 425−438.
(54) Comunas, M. J. P.; Paredes, X.; Gacino, F. M.; Fernandez, J.; Bazile, J.-P.; Boned, C.; Daridon, J. L.; Galliero, G.; Pauly, J.; Harris, K. R. Viscosity Measurements for Squalane at High Pressures to 350 MPa from T = (293.15 to 363.15) K. *J. Chem. Thermodyn.* **2014**, *69*, 201−208.
(55) Bøhling, L.; Veldhorst, A. A.; Ingebrigtsen, T. S.; Bailey, N. P.; Hansen, J. S.; Toxvaerd, S.; Schrøder, T. B.; Dyre, J. C. Do the

Repulsive and Attractive Pair Forces Play Separate Roles for the Physics of Liquids? *J. Phys.: Condens. Matter* **2013**, *25*, 032101.
(56) Kob, W.; Andersen, H. C. Testing Mode-Coupling Theory for a Supercooled Binary Lennard-Jones Mixture I: The van Hove Correlation Function. *Phys. Rev. E* **1995**, *51*, 4626−4641.
(57) Malins, A.; Eggers, J.; Royall, C. P. Investigating Isomorphs with the Topological Cluster Classification. *J. Chem. Phys.* **2013**, *139*, 234505.
(58) Roland, C. M. Relaxation Phenomena in Vitrifying Polymers and Molecular Liquids. *Macromolecules* **2010**, *43*, 7875−7890.
(59) Gallington, L. C.; Bongiorno, A. Thermodynamic Stability Limits of Simple Monoatomic Materials. *J. Chem. Phys.* **2010**, *132*, 174707.
(60) Urban, S.; Roland, C. M. Low Frequency Relaxation in Liquid Crystals in Relation to Structural Relaxation in Glass-Formers. *J. Non-Cryst. Solids* **2011**, *357*, 740−745.
(61) Alba-Simionesco, C.; Cailliaux, A.; Alegria, A.; Tarjus, G. Scaling out the Density Dependence of the Alpha Relaxation in Glass-Forming Polymers. *Europhys. Lett.* **2004**, *68*, 58−64.
(62) Papathanassiou, A. N. Density Scaling of the Diffusion Coefficient at Various Pressures in Viscous Liquids. *Phys. Rev. E* **2009**, *79*, 032501.
(63) Papathanassiou, A. N.; Sakellis, I. Correlation of the Scaling Exponent Gamma of the Diffusivity-Density Function in Viscous Liquids with their Elastic Properties. *J. Chem. Phys.* **2010**, *132*, 154503.
(64) Papathanassiou, A. N. A Plausible Interpretation of the Density Scaling of the Diffusivity in Viscous Liquids. *J. Non-Cryst. Solids* **2011**, *357*, 401−403.
(65) Wang, L.; Xu, N. Probing the Glass Transition from Structural and Vibrational Properties of Zero-Temperature Glasses. *Phys. Rev. Lett.* **2014**, *112*, 055701.
(66) Xu, W.-S.; Freed, K. F. Thermodynamic Scaling of Dynamics in Polymer Melts: Predictions from the Generalized Entropy Theory. *J. Chem. Phys.* **2013**, *138*, 234501.
(67) Kivelson, D.; Tarjus, G.; Zhao, X.; Kivelson, S. A. Fitting of Viscosity: Distinguishing the Temperature Dependences Predicted by Various Models of Supercooled Liquids. *Phys. Rev. E* **1996**, *53*, 751−758.
(68) Alba-Simionesco, C.; Kivelson, D.; Tarjus, G. Temperature, Density, and Pressure Dependence of Relaxation Times in Supercooled Liquids. *J. Chem. Phys.* **2002**, *116*, 5033−5038.
(69) Tölle, A. Neutron Scattering Studies of the Model Glass Former Ortho-Terphenyl. *Rep. Prog. Phys.* **2001**, *64*, 1473−1532.
(70) Roland, C. M.; Casalini, R.; Paluch, M. Isochronal Temperature−Pressure Superpositioning of the Alpha−Relaxation in Type-A Glass Formers. *Chem. Phys. Lett.* **2003**, *367*, 259−264.
(71) Lubchenko, V.; Wolynes, P. G. Theory of Structural Glasses and Supercooled Liquids. *Annu. Rev. Phys. Chem.* **2007**, *58*, 235−266.
(72) Cavagna, A. Supercooled Liquids for Pedestrians. *Phys. Rep.* **2009**, *476*, 51−124.
(73) Berthier, L.; Biroli, G. Theoretical Perspective on the Glass Transition and Amorphous Materials. *Rev. Mod. Phys.* **2011**, *83*, 587−645.
(74) Ediger, M. D.; Harrowell, P. Perspective: Supercooled Liquids and Glasses. *J. Chem. Phys.* **2012**, *137*, 080901.
(75) Fragiadakis, D.; Casalini, R.; Roland, C. M. Density Scaling and Dynamic Correlations in Viscous Liquids. *J. Phys. Chem. B* **2009**, *113*, 13134−13137.
(76) Errington, J. R.; Truskett, T. M.; Mittal, J. Excess-Entropy-Based Anomalies for a Waterlike Fluid. *J. Chem. Phys.* **2006**, *125*, 244502.
(77) Mittal, J.; Errington, J. R.; Truskett, T. M. Quantitative link between single-particle dynamics and static structure of supercooled liquids. *J. Phys. Chem. B* **2006**, *110*, 18147−18150.
(78) Ruchi, S.; Chakraborty, S. N.; Chakravarty, C. Entropy, Diffusivity, and Structural Order in Liquids with Waterlike Anomalies. *J. Chem. Phys.* **2006**, *125*, 204501.
(79) Abramson, E. H.; West-Foyle, H. Viscosity of Nitrogen Measured to Pressures of 7 GPa and Temperatures of 573 K. *Phys. Rev. E* **2008**, *77*, 041202.
(80) Abramson, E. H. Viscosity of Methane to 6 GPa and 673 K. *Phys. Rev. E* **2011**, *84*, 062201.
(81) Agarwal, M.; Singh, M.; Sharma, R.; Alam, M. P.; Chakravarty, C. Relationship between Structure, Entropy, and Diffusivity in Water and Water-like Liquids. *J. Phys. Chem. B* **2010**, *114*, 6995−7001.
(82) Fomin, Y. D.; Ryzhov, V. N.; Gribova, N. V. Breakdown of Excess Entropy Scaling for Systems with Thermodynamic Anomalies. *Phys. Rev. E* **2010**, *81*, 061201.
(83) Chopra, R.; Truskett, T. M.; Errington, J. R. On the Use of Excess Entropy Scaling to Describe Single-Molecule and Collective Dynamic Properties of Hydrocarbon Isomer Fluids. *J. Phys. Chem. B* **2010**, *114*, 16487−16493.
(84) Pond, M. J.; Errington, J. R.; Truskett, T. M. Generalizing Rosenfeld's Excess-Entropy Scaling to Predict Long-Time Diffusivity in Dense Fluids of Brownian Particles: From Hard to Ultrasoft Interactions. *J. Chem. Phys.* **2011**, *134*, 081101.
(85) Pond, M. J.; Errington, J. R.; Truskett, T. M. Mapping between Long-Time Molecular and Brownian Dynamics. *Soft Matter* **2011**, *7*, 9859−9862.
(86) Helge-Otmar, M.; Mausbach, P. Thermodynamic Excess Properties and their Scaling Behavior for the Gaussian Core Model Fluid. *Fluid Phase Equilib.* **2012**, *313*, 156−164.
(87) Coslovich, D.; Ikeda, A. Cluster and Reentrant Anomalies of Nearly Gaussian Core Particles. *Soft Matter* **2013**, *9*, 6786−6795.
(88) Krekelberg, W. P.; Pond, M. J.; Goel, G.; Shen, V. K.; Errington, J. R.; Truskett, T. M. Generalized Rosenfeld Scalings for Tracer Diffusivities in Not-so-Simple Fluids: Mixtures and Soft Particles. *Phys. Rev. E* **2009**, *80*, 061205.
(89) Pond, M. J.; Krekelberg, W. P.; Shen, V. K.; Errington, J. R.; Truskett, T. M. Composition and Concentration Anomalies for Structure and Dynamics of Gaussian-Core Mixtures. *J. Chem. Phys.* **2009**, *131*, 161101.
(90) Dzugutov, M. A Universal Scaling Law for Atomic Diffusion in Condensed Matter. *Nature* **1996**, *381*, 137−139.
(91) Truskett, T. M.; Torquato, S.; Debenedetti, P. G. Towards a Quantification of Disorder in Materials: Distinguishing Equilibrium and Glassy Sphere Packings. *Phys. Rev. E* **2000**, *62*, 993−1001.
(92) Errington, J. R.; Debenedetti, P. G.; Torquato, S. Quantification of Order in the Lennard-Jones System. *J. Chem. Phys.* **2003**, *118*, 2256−2263.
(93) Shell, M. S.; Debenedetti, P. G.; Panagiotopoulos, A. Z. Molecular Structural Order and Anomalies in Liquid Silica. *Phys. Rev. E* **2002**, *66*, 011202.
(94) Errington, J. R.; Debenedetti, P. G. Relationship between Structural Order and the Anomalies of Liquid Water. *Nature* **2001**, *409*, 318−321.
(95) Giovambattista, N.; Debenedetti, P. G.; Sciortino, F.; Stanley, H. E. Structural Order in Glassy Water. *Phys. Rev. E* **2005**, *71*, 061505.
(96) Ellegaard, N. L.; Christensen, T.; Christiansen, P. V.; Olsen, N. B.; Pedersen, U. R.; Schrøder, T. B.; Dyre, J. C. Single-Order-Parameter Description of Glass-Forming Liquids: A One-Frequency Test. *J. Chem. Phys.* **2007**, *126*, 074502.
(97) Pick, R. M. The Prigogine-Defay Ratio and the Microscopic Theory of Supercooled Liquids. *J. Chem. Phys.* **2008**, *129*, 124115.
(98) Ribeiro, M. C. C.; Scopigno, T.; Ruocco, G. Prigogine-Defay Ratio for an Ionic Glass-Former: Molecular Dynamics Simulations. *J. Phys. Chem. B* **2009**, *113*, 3099−3104.
(99) Lion, A.; Peters, J. Coupling Effects in Dynamic Calorimetry: Frequency-Dependent Relations for Specific Heat and Thermomechanical Responses - A One-Dimensional Approach based on Thermodynamics with Internal State Variables. *Thermochim. Acta* **2010**, *500*, 76−87.
(100) Garden, J.-L.; Guillou, H.; Richard, J.; Wondraczek, L. Non-Equilibrium Configurational Prigogine-Defay Ratio. *J. Non-Equilib. Thermodyn.* **2012**, *37*, 143−177.
(101) Christensen, T.; Jakobsen, B.; Papini, J.; Hecksher, T.; Dyre, J. C.; Olsen, N. B. A Combined Measurement of Thermal and Mechanical Relaxation. *J. Non-Cryst. Solids* **2011**, *357*, 346−350.

(102) Gundermann, D.; Pedersen, U. R.; Hecksher, T.; Bailey, N. P.; Jakobsen, B.; Christensen, T.; Olsen, N. B.; Schrøder, T. B.; Fragiadakis, D.; Casalini, R.; Roland, C. M.; Dyre, J. C.; Niss, K. Predicting the Density–Scaling Exponent of a Glass–Forming Liquid from Prigogine–Defay Ratio Measurements. *Nat. Phys.* **2011**, *7*, 816–821.
(103) Angell, C. A.; Klein, I. S. Prigogine and Defay say Relax. *Nat. Phys.* **2011**, *7*, 750–751.
(104) Casalini, R.; Gamache, R. F.; Roland, C. M. Density-Scaling and the Prigogine-Defay Ratio in Liquids. *J. Chem. Phys.* **2011**, *135*, 224501.
(105) Veldhorst, A. A.; Bøhling, L.; Dyre, J. C.; Schrøder, T. B. Isomorphs in the phase diagram of a model liquid without inverse power law repulsion. *Eur. Phys. J. B* **2012**, *85*, 21.
(106) Krekelberg, W. P.; Mittal, J.; Ganesan, V.; Truskett, T. M. Structural Anomalies of Fluids: Origins in Second and Higher Coordination Shells. *Phys. Rev. E* **2008**, *77*, 041201.
(107) Singh, M.; Dhabal, D.; Nguyen, A. H.; Molinero, V.; Chakravarty, C. Triplet Correlations Dominate the Transition from Simple to Tetrahedral Liquids. *Phys. Rev. Lett.* **2014**, *112*, 147801.
(108) Adam, G.; Gibbs, J. H. On Temperature Dependence of Cooperative Relaxation Properties in Glass-Forming Liquids. *J. Chem. Phys.* **1965**, *43*, 139–146.
(109) Betancourt, B. A. P.; Douglas, J. F.; Starr, F. W. Fragility and Cooperative Motion in a Glass-Forming Polymer-Nanoparticle Composite. *Soft Matter* **2013**, *9*, 241–254.
(110) Sengupta, S.; Schrøder, T. B.; Sastry, S. Density-Temperature Scaling of the Fragility in a Model Glass-Former. *Eur. Phys. J. E* **2013**, *36*, 113.
(111) Rosenfeld, Y.; Tarazona, P. Density Functional Theory and the Asymptotic High Density Expansion of the Free Energy of Classical Solids and Fluids. *Mol. Phys.* **1998**, *95*, 141–150.
(112) Ingebrigtsen, T. S.; Veldhorst, A. A.; Schrøder, T. B.; Dyre, J. C. Communication: The Rosenfeld-Tarazona Expression for Liquids' Specific Heat: A Numerical Investigation of Eighteen Systems. *J. Chem. Phys.* **2013**, *139*, 171101.
(113) Ingebrigtsen, T. S.; Errington, J. R.; Truskett, T. M.; Dyre, J. C. Predicting How Nanoconfinement Changes the Relaxation Time of a Supercooled Liquid. *Phys. Rev. Lett.* **2013**, *111*, 235901.
(114) Separdar, L.; Bailey, N. P.; Schrøder, T. B.; Davatolhagh, S.; Dyre, J. C. Isomorph Invariance of Couette Shear Flows Simulated by the SLLOD Equations of Motion. *J. Chem. Phys.* **2013**, *138*, 154505.
(115) Lerner, E.; Procaccia, I.; Ching, E. S. C.; Hentschel, H. G. E. Relations between Material Mechanical Parameters and Interparticle Potential in Amorphous Solids. *Phys. Rev. B* **2009**, *79*, 180203.
(116) Lerner, E.; Procaccia, I. Scaling Theory for Steady-State Plastic Flows in Amorphous Solids. *Phys. Rev. E* **2009**, *80*, 026128.
(117) Procaccia, I. Physics of Amorphous Solids: Their Creation and their Mechanical Properties. *Eur. Phys. J. Spec. Top.* **2009**, *178*, 81–122.
(118) Lerner, E.; Bailey, N. P.; Dyre, J. C. Density Scaling and Quasiuniversality of Flow-Event Statistics for Athermal Plastic Flows. 2014, arXiv:1405.0156.
(119) Rice, S. A.; Gray, P. *The Statistical Mechanics of Simple Liquids*; Interscience: New York, 1965.
(120) Temperley, H. N. V.; Rowlinson, J. S.; Rushbrooke, G. S. *Physics of Simple Liquids*; Wiley: New York, 1968.
(121) Barrat, J.-L.; Hansen, J.-P. *Basic Concepts for Simple and Complex Liquids*; Cambridge University Press: United Kingdom, 2003.
(122) Debenedetti, P. G. Structure, Dynamics and Thermodynamics in Complex Systems: Theoretical Challenges and Opportunities. *AIChE J.* **2005**, *51*, 2391–2395.
(123) Bagchi, B.; Chakravarty, C. Interplay between Multiple Length and Time Scales in Complex Chemical Systems. *J. Chem. Sci.* **2010**, *122*, 459–470.
(124) Mausbach, P.; May, H.-O. Direct Molecular Simulation of the Grüneisen Parameter and Density Scaling Exponent in Fluid Systems. *Fluid Phase Equilib.* **2014**, *366*, 108–116.
(125) Debenedetti, P. G. Supercooled and Glassy Water. *J. Phys.: Condens. Matter* **2003**, *15*, R1669–R1726.
(126) Dyre, J. C. The Glass Transition and Elastic Models of Glass-Forming Liquids. *Rev. Mod. Phys.* **2006**, *78*, 953–972.
(127) Dyre, J. C.; Wang, W. H. The Instantaneous Shear Modulus in the Shoving Model. *J. Chem. Phys.* **2012**, *136*, 224108.
(128) Mirigian, S.; Schweizer, K. S. Unified Theory of Activated Relaxation in Liquids over 14 Decades in Time. *J. Phys. Chem. Lett.* **2013**, *4*, 3648–3653.
(129) Mittal, J.; Errington, J. R.; Truskett, T. M. Thermodynamics Predicts how Confinement Modifies the Dynamics of the Equilibrium Hard-Sphere Fluid. *Phys. Rev. Lett.* **2006**, *96*, 177804.
(130) Berthier, L.; Tarjus, G. Nonperturbative Effect of Attractive Forces in Viscous Liquids. *Phys. Rev. Lett.* **2009**, *103*, 170601.
(131) Berthier, L.; Tarjus, G. The Role of Attractive Forces in Viscous Liquids. *J. Chem. Phys.* **2011**, *134*, 214503.
(132) Fragiadakis, D.; Roland, C. M. Connection between Dynamics and Thermodynamics of Liquids on the Melting Line. *Phys. Rev. E* **2011**, *83*, 031504.
(133) Roland, C. M. Density Scaling of the Structural and Johari-Goldstein Secondary Relaxations in Poly(methyl methacrylate). *Macromolecules* **2013**, *46*, 6364–6368.
(134) Hensel-Bielowka, S.; Sangoro, J. R.; Wojnarowska, Z.; Hawelek, L.; Paluch, M. The Behavior and Origin of the Excess Wing in DEET (N,N-diethyl-3-methylbenzamide). *Phys. Chem. Chem. Phys.* **2013**, *15*, 9300–9307.
(135) Ngai, K. L.; Habasaki, J.; Prevosto, D.; Capaccioli, S.; Paluch, M. Thermodynamic Scaling of α-Relaxation Time and Viscosity Stems from the Johari-Goldstein β-Relaxation or the Primitive Relaxation of the Coupling Model. *J. Chem. Phys.* **2012**, *137*, 034511.
(136) Koperwas, K.; Grzybowski, A.; Grzybowska, K.; Wojnarowska, Z.; Sokolov, A. P.; Paluch, M. Effect of Temperature and Density Fluctuations on the Spatially Heterogeneous Dynamics of Glass-Forming van der Waals Liquids under High Pressure. *Phys. Rev. Lett.* **2013**, *111*, 125701.
(137) Grzybowski, A.; Koperwas, K.; Kolodziejczyk, K.; Grzybowska, K.; Paluch, M. Spatially Heterogeneous Dynamics in the Density Scaling Regime: Time and Length Scales of Molecular Dynamics near the Glass Transition. *J. Phys. Chem. Lett.* **2013**, *4*, 4273–4278.
(138) Bailey, N. P.; Schrøder, T. B.; Dyre, J. C. Variation of the Dynamic Susceptibility along an Isochrone. 2014, arXiv:1404.7706.
(139) Grzybowski, A.; Grzybowska, K.; Paluch, M.; Swiety, A.; Koperwas, K. Density scaling in viscous systems near the glass transition. *Phys. Rev. E* **2011**, *83*, 041505.
(140) Lopez, E. R.; Pensado, A. S.; Fernandez, J.; Harris, K. R. On the Density Scaling of pVT Data and Transport Properties for Molecular and Ionic Liquids. *J. Chem. Phys.* **2012**, *136*, 214502.
(141) Grzybowski, A.; Koperwas, K.; Swiety-Pospiech, A.; Grzybowska, K.; Paluch, M. Activation Volume in the Density Scaling Regime: Equation of State and its Test by Using Experimental and Simulation Data. *Phys. Rev. B* **2013**, *87*, 054105.
(142) Schrøder, T. B.; Gnan, N.; Pedersen, U. R.; Bailey, N. P.; Dyre, J. C. Pressure-Energy Correlations in Liquids. V. Isomorphs in Generalized Lennard-Jones Systems. *J. Chem. Phys.* **2011**, *134*, 164505.
(143) Elmatad, Y. S.; Chandler, D.; Garrahan, J. P. Corresponding States of Structural Glass Formers. II. *J. Phys. Chem. B* **2010**, *114*, 17113–17119.
(144) Fragiadakis, D.; Roland, C. M. Are Polar Liquids less Simple? *J. Chem. Phys.* **2013**, *138*, 12A502.
(145) Budzien, J.; Heffernan, J. V.; McCoy, J. D. Effect of Chain Flexibility on Master Curve Behavior for Diffusion Coefficient. *J. Chem. Phys.* **2013**, *139*, 244501.
(146) Voyiatzis, E.; Muller-Plathe, F.; Bohm, M. C. Do Transport Properties of Entangled Linear Polymers Scale with Excess Entropy? *Macromolecules* **2013**, *46*, 8710–8723.
(147) Lopez-Flores, L.; Ruiz-Estrada, H.; Chavez-Paez, M.; Medina-Noyola, M. Dynamic Equivalences in the Hard-Sphere Dynamic Universality Class. *Phys. Rev. E* **2013**, *88*, 042301.
(148) Khrapak, S. A.; Chaudhuri, M.; Morfill, G. E. Communication: Universality of the Melting Curves for a Wide Range of Interaction Potentials. *J. Chem. Phys.* **2011**, *134*, 241101.

(149) Shi, Z.; Debenedetti, P. G.; Stillinger, F. H.; Ginart, P. Structure, Dynamics, and Thermodynamics of a Family of Potentials with Tunable Softness. *J. Chem. Phys.* **2011**, *135*, 084513.
(150) Biroli, G.; Karmakar, S.; Procaccia, I. Comparison of Static Length Scales Characterizing the Glass Transition. *Phys. Rev. Lett.* **2013**, *111*, 165701.
(151) Karmakar, S.; Dasgupta, C.; Sastry, S. Growing Length Scales and Their Relation to Timescales in Glass-Forming Liquids. *Annu. Rev. Condens. Matter Phys.* **2014**, *5*, 255−284.
(152) Ramirez-Gonzalez, P. E.; Lopez-Flores, L.; Acuna-Campa, H.; Medina-Noyola, M. Density-Temperature-Softness Scaling of the Dynamics of Glass-Forming Soft-Sphere Liquids. *Phys. Rev. Lett.* **2011**, *107*, 155701.
(153) Schmiedeberg, M.; Haxton, T. K.; Nagel, S. R.; Liu, A. J. Mapping the Glassy Dynamics of Soft Spheres onto Hard-Sphere Behavior. *EPL* **2011**, *96*, 36010.
(154) Rodriguez-Lopez, T.; Moreno-Razo, J.; del Rio, F. Thermodynamic Scaling and Corresponding States for the Self-Diffusion Coefficient of Non-Conformal Soft-Sphere Fluids. *J. Chem. Phys.* **2013**, *138*, 114502.
(155) Papini, J. J.; Schrøder, T. B.; Dyre, J. C. Do all Liquids Become Strongly Correlating at High Pressure? 2011, arXiv:1103.4954.